

STRAIN RATE BEHAVIOUR
OF SAINT - JEAN - VIANNEY
CLAY

by

PETER K. ROBERTSON

B.Sc., University of Nottingham, 1972.

A THESIS SUBMITTED IN PARTIAL FULFILMENT OF
THE REQUIREMENTS FOR THE DEGREE OF
MASTER OF APPLIED SCIENCE

in the Department
of
CIVIL ENGINEERING

We accept this thesis as conforming to the
required standard

THE UNIVERSITY OF BRITISH COLUMBIA

May, 1975.

In presenting this thesis in partial fulfilment of the requirements for an advanced degree at the University of British Columbia, I agree that the Library shall make it freely available for reference and study. I further agree that permission for extensive copying of this thesis for scholarly purposes may be granted by the Head of my Department or by his representatives. It is understood that copying or publication of this thesis for financial gain shall not be allowed without my written permission.

Department of CIVIL ENGINEERING.

The University of British Columbia
Vancouver 8, Canada

Date April 1975.

ABSTRACT

A series of constant rate of strain compression tests and creep rupture tests have been performed on undisturbed, isotropically consolidated quick clay from the Saint-Jean-Vianney region, Quebec Province, Canada. Both drained and undrained tests were performed in conventional triaxial equipment. Also included is the data obtained from a series of K_0 consolidation tests performed by Dr. Y.P. Vaid at U.B.C.

Saint-Jean-Vianney clay, hereafter referred to as S.J.V. clay, is a stiff, heavily overconsolidated, cemented clay, from the site of the Saint-Jean-Vianney slide of 1971.

The testing of this very stiff, cemented clay proved to be very difficult due to its very stiff and brittle nature, combined with its lenses of silt and fine sand. The consolidation testing showed that the preconsolidation pressure could vary from 7.5 Kg/cm^2 to 12 Kg/cm^2 depending on the strain rate of the test.

Snead (1970) and Campanella and Vaid (1972) performed similar creep tests on a local clay, known as Haney clay. The analysis of the creep tests performed on S.J.V. clay showed similar relationships to those reported by Snead and, Campanella and Vaid, but because of the extremely stiff nature of this clay the scatter

of the results was more than that reported for Haney clay. The testing indicated a possible stress-strain-strain rate relationship may exist along with a possible drained failure criterion.

The results obtained from this research were very dependant on the bonding of this clay, and indicate that the bond strength appears to be a function of strain rate.

TABLE OF CONTENTS

CHAPTER		Page
I	INTRODUCTION	
	1.1 Introduction	1
	1.2 Review of Literature	2
	Creep and Creep Rupture	2
	Quick Clays of Eastern	10
	1.3 Scope	18
2	LABORATORY TESTING	
	2.1 Description of Soil Tested	21
	2.2 Description of Apparatus	23
	2.3 Experimental Procedure	25
	Sample Preparation	25
	Constant Rate of Strain	
	Compression Tests	26
	Creep Tests	27
3	EFFECTS OF STRAIN RATE ON CONSOLIDATION	30
4	RESULTS AND DISCUSSION OF CONSTANT RATE OF STRAIN COMPRESSION TESTS	
	4.1 Undrained Constant rate of Strain Compression Tests	34
	4.2 Drained Constant Rate of Strain Compression Tests	40

CHAPTER		Page
5	RESULTS AND DISCUSSION OF CREEP TESTS	
	5.1 Undrained Creep Tests	52
	5.2 Drained Creep Tests	61
	5.3 Stress-Strain-Strain Rate Relations	65
	5.4 Effective Stress Conditions	70
6	SUMMARY AND CONCLUSIONS	73
	BIBLIOGRAPHY	75
	APPENDIX I Calculation of Strain Rates	78
	II Sketches of Failed Samples	80

LIST OF TABLES.

Table		Page
I	Physical properties of undisturbed S.J.V. clay.	22
II	Summary of test information for strain controlled compression tests.	28
III	Summary of test information for the creep tests.	29
IV	Summary of results of strain controlled compression tests.	51
V	Summary of results of creep tests.	66

LIST OF FIGURES.

Figure		Page
1.	A typical strain-time curve for normally consolidated Haney clay under sustained deviator stress. (After Snead, 1970)	4
2.	Logarithm of axial strain rate versus Log. elapsed time for normally consolidated undrained creep tests on Haney clay. (After Snead, 1970)	5
3.	Minimum strain rate against total rupture life. (After Snead, 1970)	7
4.	Relationship between time to rupture and current strain rate. (After Snead, 1970)	9
5.	Effective stress conditions at creep rupture and minimum creep rate. (After Campanella & Vaid, 1972)	11
6.	Area of Eastern Canada where Leda clay is found.	13
7.	Schematic of the development of cementation bonds and frictional strengths and the observed composite shapes. (After Conlon, 1966)	15

Figure	Page
8. Typical Mohr-Coulomb plot for consolidated drained triaxial tests on Leda clay. (After Conlon, 1966)	17
9. Typical compression log pressure curves for various rates of loading. (After Crawford, 1967)	19
10. Schematic layout of loading, displacement, pressure and volume change measuring system.	24
11. Change in void ratio against vertical effective stress for K_0 consolidation tests on undisturbed S.J.V. Clay at different strain rates.	31
12. Plot of the coefficient of consolidation against vertical effective stress for K_0 consolidation tests on undisturbed S.J.V. clay at different strain rates.	33
13. Isotropic triaxial constant rate of strain undrained tests on top layer of undisturbed S.J.V. clay.	35
14. Change in pore pressure during constant rate of strain undrained, undrained compression tests on top layer of undisturbed S.J.V. clay.	36

Figure	Page
15. Isotropic triaxial constant rate of strain undrained tests on lower layer of undisturbed S.J.V. clay.	38
16. Change in pore pressure during constant rate of strain, undrained compression tests on lower layer of undisturbed S.J.V. clay.	39
17. Isotropic triaxial constant rate of strain drained test on undisturbed S.J.V. clay.	41
18. Volumetric strain during constant rate of strain drained test on undisturbed S.J.V. clay.	42
19. Isotropic triaxial constant rate of strain undrained/drained test on undisturbed S.J.V. clay.	44
20. Volumetric strain and change in pore pressure during undrained/drained test on undisturbed S.J.V. clay.	45
21. Comparision between drained and undrained isotropic triaxial constant rate of strain tests on undisturbed S.J.V. clay.	46

Figure	Page
22. Typical stress path for strain controlled undrained compression tests.	48
23. Effective stress condition for strain controlled compression tests at peak and final deviator conditions.	49
24. Creep rate behaviour for isotropically consolidated, undisturbed S.J.V. clay under symmetric loading.	53
25. Relationship between rupture life and minimum creep rate for isotropically consolidated undisturbed S.J.V. clay.	55
26. Relationship between minimum creep rate and remaining time to rupture for isotropically consolidated undisturbed S.J.V. clay.	56
27. Some typical curves for Teriary creep rate against remaining time to rupture, tt_r , for isotropically consolidated undisturbed S.J.V. clay.	58
28. Relationship between minimum creep rate and stress level for both layers of the block sample of S.J.V. clay.	59

Figure	Page
29. Relationship between peak deviator stress and strain rate for undrained strain controlled tests on both layers of the block sample of S.J.V. clay.	60
30. Variation of creep strength with time to rupture for isotropically consolidated S.J.V. clay.	62
31. Creep rate behaviour for isotropically consolidated drained creep tests on undisturbed S.J.V. clay.	64
32. Relationship between strain rate and strain for some of the undrained S.J.V. clay.	67
33. Comparison of observed stress-strain behaviour in undrained constant strain rate compression tests with that predicted from undrained creep tests.	69
34. Effective stress conditions at minimum creep rate for the undrained creep tests on undisturbed S.J.V. clay.	71

LIST OF SYMBOLS

$\sigma_{1,2,3}$	Principal total stresses
$\sigma'_{1,2,3}$	Principal effective stresses
K_0	Coefficient of earth pressure at rest
σ_0	Deviator stress ($\sigma_1 - \sigma_3$)
t	Elapsed time
t_m	Time to minimum strain rate
t_r	Total rupture life
tt_r	Time to rupture
$\dot{\epsilon}_s$	Secondary creep strain rate
$\dot{\epsilon}_m$	Minimum strain rate
τ	Shear stress
σ'	Effective stress
t_f	Time to failure
c_v	Coefficient of consolidation
u	Pore pressure
A & B	Skempton's pore pressure parameters
A_f	Pore pressure parameter at failure

ACKNOWLEDGEMENTS

The writer would like to thank his research supervisor, Dr.R.G. Campanella for his guidance during this research. He further wishes to express his appreciation to Dr.P.M. Byrne for his valuable suggestions.

The writer also wishes to express his gratitude to Dr.Y.P. Vaid for his continued interest and advice throughout this research.

CHAPTER 1

INTRODUCTION

1.1 Introduction.

At present, 1975, Limit Design is used for most soil mechanics problems involving the strength and stability of slopes. Although providing a means for design against total collapse, it does not estimate the magnitude of anticipated deformations, especially with respect to time.

The influence of time on stress/strain relations has been observed under field conditions by many, including Haefeli (1953), Saito and Uezawa (1961) and Suklje (1961). They report continual movements taking place in natural slopes in which the total stresses are remaining nearly constant. These time dependent shearing deformations have given the engineer many difficulties as he is unable to predict reliably the long term behaviour.

This problem is particularly true of slopes in the very sensitive clays of Eastern Canada. Such slides as the one that occurred at Saint - Jean - Vianney, Quebec, on May 4th, 1971, where an estimated 9×10^6 cubic yards of material moved from an area of approximately 350,000 square yards, Tavenas (1971).

With the availability of a block sample from this actual slide site, it was felt there was an ideal opportunity for an investigation into the strain rate behaviour of this very stiff, very sensitive, heavily over consolidated clay.

1.2 Review of Literature.

This literature review will present the pertinent information on creep and creep rupture and also a general review of the characteristics of the very sensitive clays of eastern Canada.

Creep and Creep Rupture.

Casagrande and Wilson (1951) have shown that some types of brittle undisturbed clays and clay shales continuously deform under sustained load, and that failure ultimately occurs under a sustained load appreciably less than the strength indicated by a normal undrained compression test. Vialor and Skibitsky (1957) investigated the effect of creep in frozen soils and showed the existence of a upper yield strength defined as the maximum sustained shearing stress which would not cause failure with time.

Snead (1970) performed creep tests on a undrained normally consolidated undisturbed sensitive clay, called Haney clay, using the conventional triaxial apparatus. A typical strain time curve is

given in Fig.1. He observed that the strain rate initially decreased, reached a minimum, and then increased gradually proceeding to rupture. He could not find a stage when the strain rate was constant, as found for metal, concrete and plastic. Snead concluded that once a minimum strain rate is reached, the sample will eventually rupture and failure can be considered to have occurred. He also confirmed the existence of an upper yield strength.

Snead (1970) obtained a log log plot of strain rate and time, as shown in Fig. 2, by performing a series of creep rupture tests with different sustained shearing stresses using the conventional triaxial apparatus. All the samples were isotropically consolidated to an effective stress of 75 psi (approximately 5.25 Kg/cm^2). Figure 2 shows that for deviator creep stresses greater than 43.4 psi, the strain rate initially decreased, reached a minimum then increased rapidly proceeding to rupture. For the sample with a deviator stress of 42.8 psi the curve appears to be proceeding towards the line of minimum strain rates but changes its course and continues parallel to the line of minimum strain rates. Thus it would appear that the stress level of 42.8 psi was below the upper yield strength of that sample. Snead used the existence of a minimum strain rate as a failure criterion, since if a

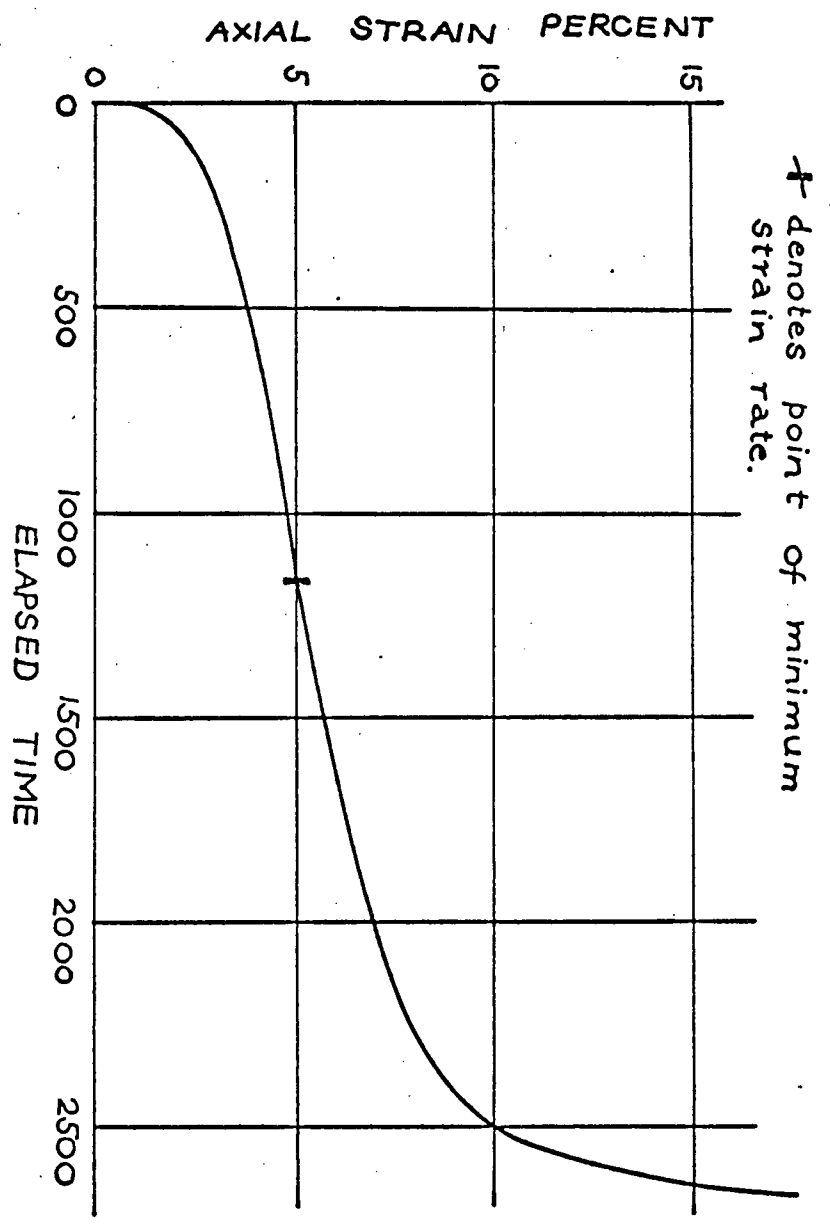


Fig. 1. A TYPICAL STRAIN-TIME CURVE FOR NORMALLY CONSOLIDATED HANEY CLAY UNDER SUSTAINED DEVIATOR STRESS. (AFTER SNEAD, 1970).

+ DENOTES POINTS OF MINIMUM STRAIN RATES

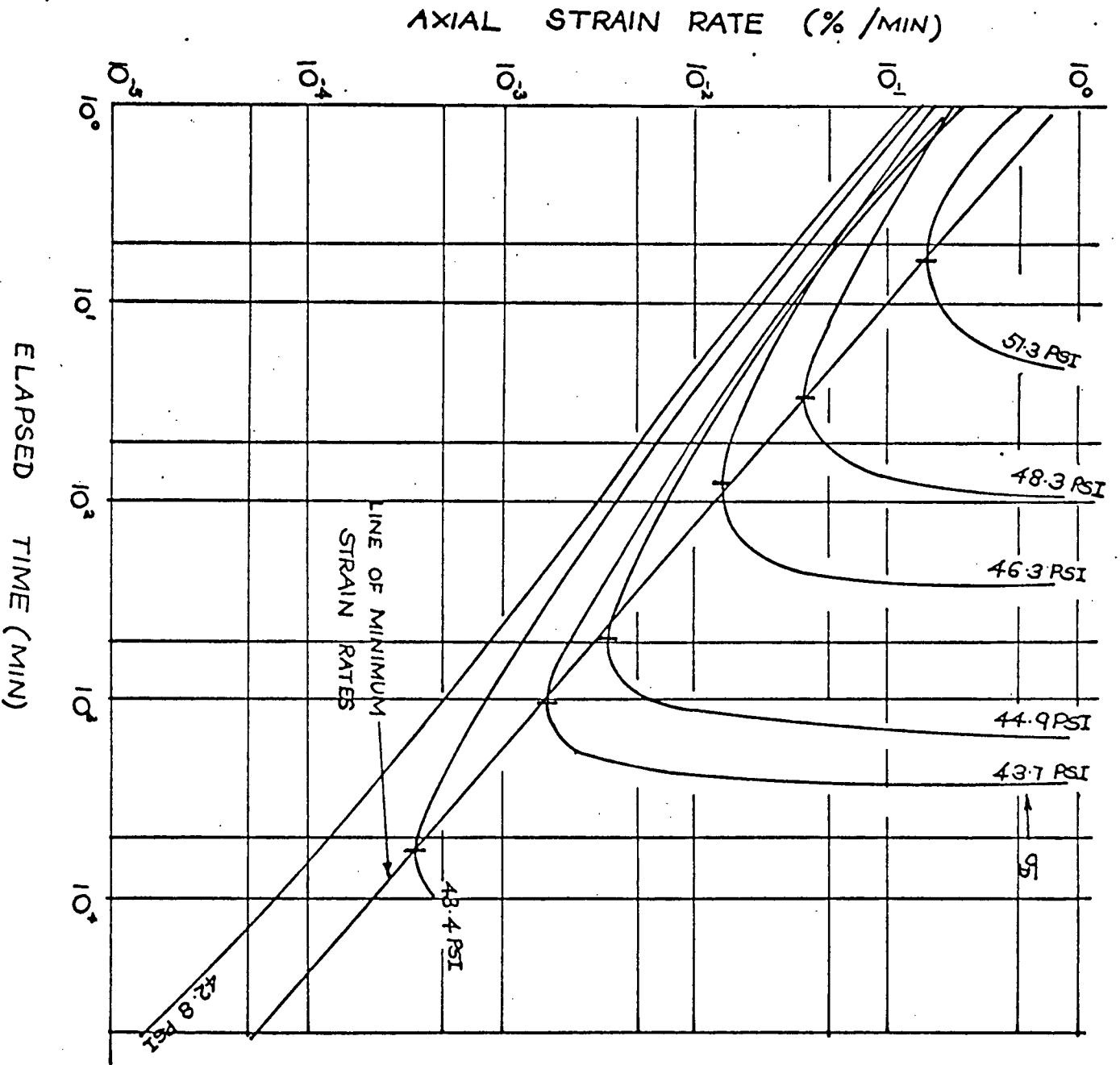


Fig. 2. LOGARITHM OF AXIAL STRAIN RATE
 VERSUS LOG. ELAPSED TIME FOR
 NORMALLY CONSOLIDATED UNDRAINED
 CREEP TESTS ON HANEY CLAY. (AFTER SNEAD,
 1970)

sample reached a minimum strain rate the sample would eventually rupture.

Saito and Uezawa (1961) performed triaxial compression tests on four Japanese soils and proposed a linear relationship between the log of secondary strain rate and the log of the total time to rupture. Snead (1970) found that a secondary creep stage did not exist for Haney clay, and suggested that the secondary strain rate measured by Saito and Uezawa was approximately equal to the minimum strain rate calculated by him. Snead also found that a linear relationship existed between the log of minimum strain rate " $\dot{\epsilon}_{\min}$ " and the total rupture life " t_r ". Snead and Saito's result are shown on Figure 3. Saito and Uezawa proposed that the relationship between " t_r " and " $\dot{\epsilon}_{\min}$ " is unique for all soils, whereas Snead suggested the relationship was similar for other soils but not necessarily unique for all soils.

Saito used this relationship to predict the occurrence of time to slope failures in 1965 with reasonable accuracy. Snead on the other hand proposed a method of predicting the time to slope failure for tertiary creep stage. Snead (1970) defined the "time to rupture" as the elapsed time from the instant considered until failure and obtained a linear relationship between log of time to rupture " tt_r " and current

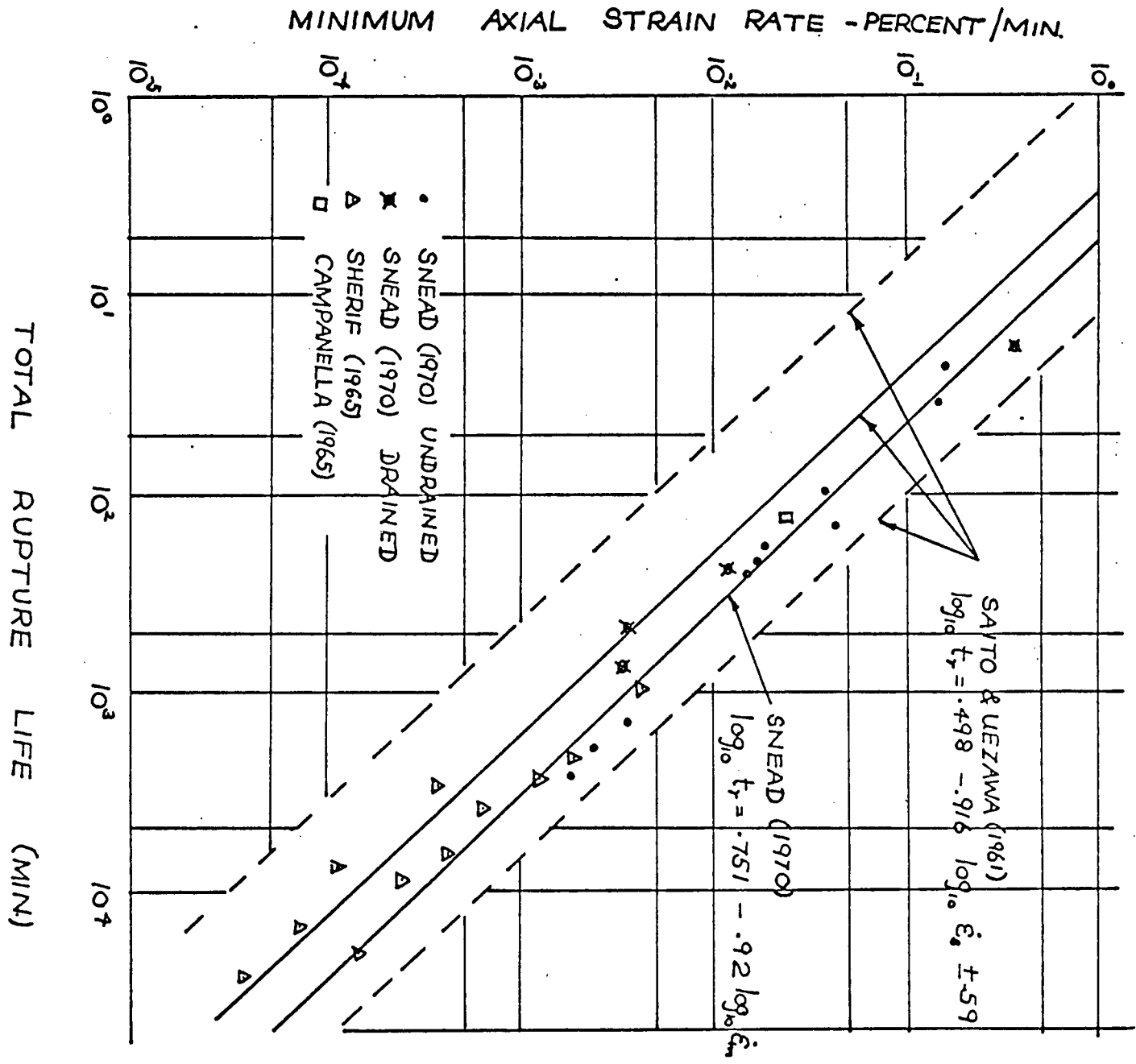


Fig. 3. MINIMUM STRAIN RATE AGAINST TOTAL RUPTURE LIFE (AFTER SNEAD, 1970)

strain rate, " $\dot{\epsilon}$ ", as shown in Figure 4.

Saito (1969) also proposed a method for predicting slope failure during tertiary creep. In this method he assumed a relationship between " t_{t_r} " and " $\dot{\epsilon}$ " similar to Figure 4, to obtain an expression for strain by mathematical intergration. He found reasonable agreement between the predicted and observed time of occurrence of slope failure.

Campanella and Vaid (1972 and 1973) tested Haney clay under constant shear stress in; K_0 consolidated triaxial, isotropically consolidated triaxial and K_0 consolidated plane strain. In comparing the results they found that the general shapes of the curves found by Snead were repeated but were shifted slightly. They found that the conventional isotropic triaxial test would give an unconservative estimate of rupture life or remaining time to rupture by a factor of about 4, if the real situation corresponded to K_0 consolidation or plane strain.

Snead (1970) and Campanella and Vaid (1972) both found a unique relationship between stress, strain and strain rate, similar to that found by Lubahn and Felgar (1961) for metals. Both restricted its use to samples tested undrained at constant temperature for continually increasing compressive axial strains, and not heavily overconsolidated. This relationship means

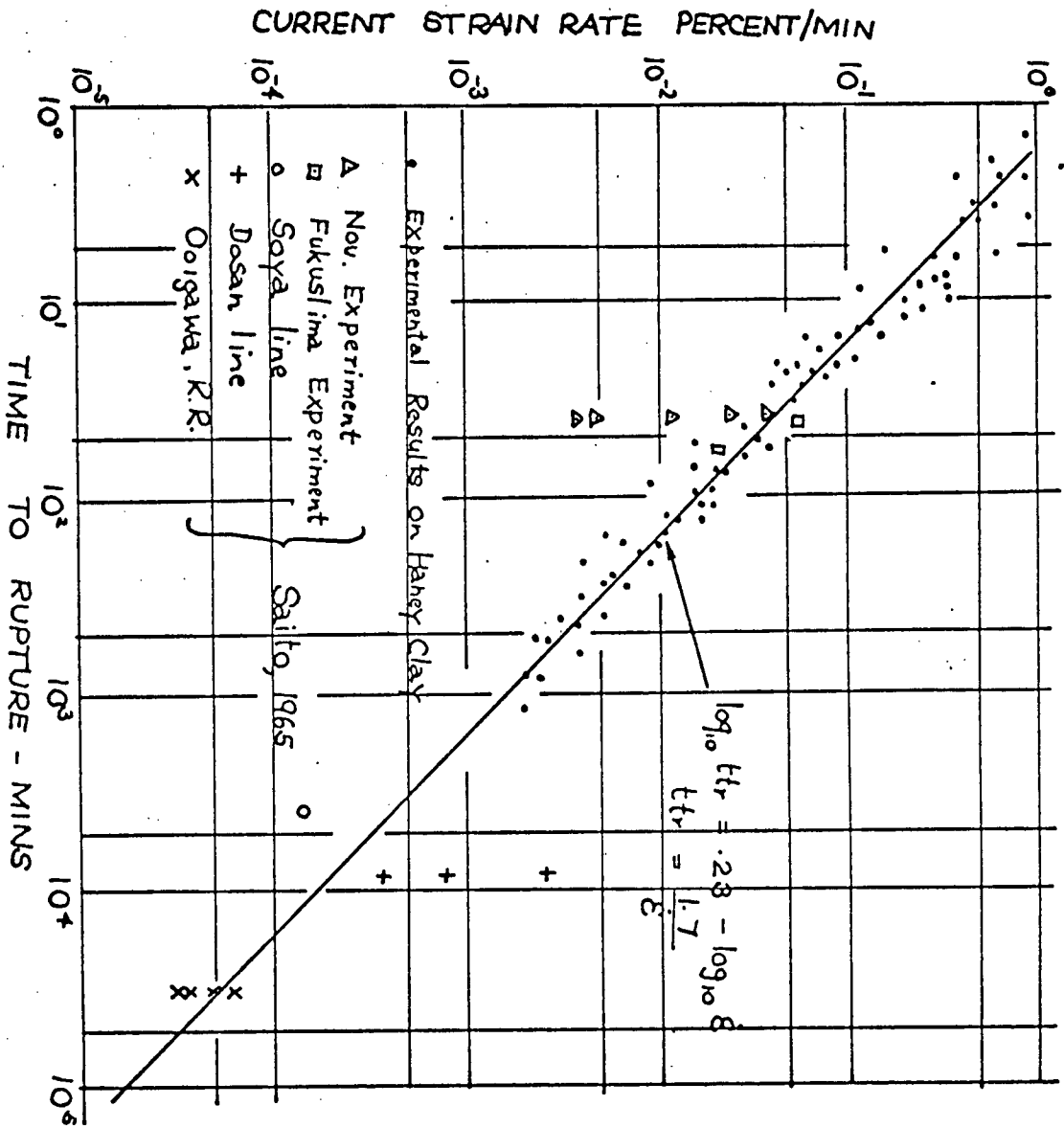


FIG. 4. RELATIONSHIP BETWEEN TIME TO RUPTURE AND CURRENT STRAIN RATE (AFTER SWEED, 1970)

that creep test curves can be obtained from stress - strain curves at different strain rates if the samples have the same consolidation history, thus creep tests and constant strain rate tests are complementary to each other for obtaining stress - strain - time properties.

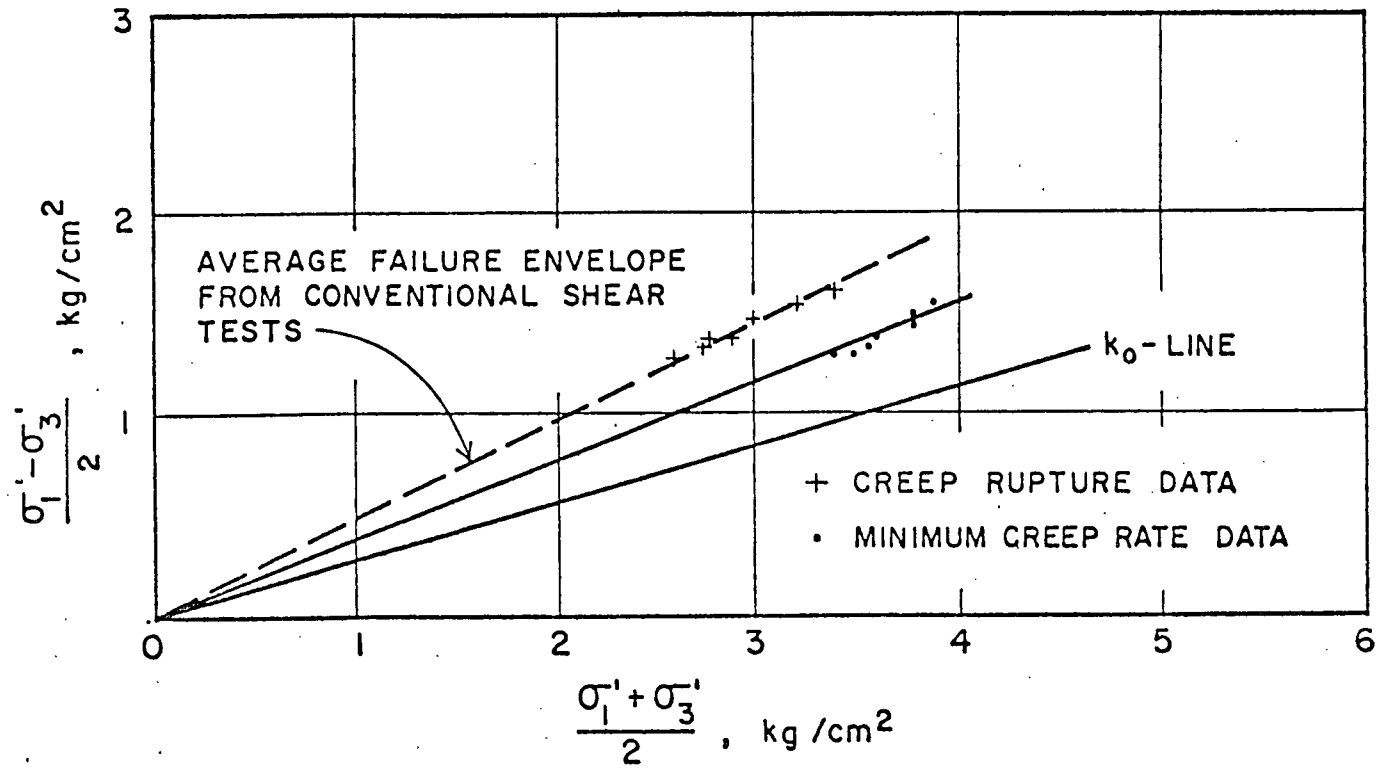
Campanella and Vaid (1972) analyzed the results of their creep rupture tests in terms of effective stresses. They obtained the same linear failure envelope for both creep rupture and failure in conventional strain rate undrained tests. This plot is shown in Figure 5. From this they could assume that the rheological component of shear resistance appeared to be negligible for that soil.

The effective stress condition at the instant when the creep rate started to increase was also shown on Figure 5, and a linear envelope passing through the origin appears to define this onset of instability. This envelope of minimum strain rates occurs at a lower shearing resistance than that defined by creep rupture and since all samples which reach this stress eventually fail, Campanella and Vaid felt it was more appropriate to use the envelope defined by the minimum creep rates as a failure criterion.

Quick Clay of Eastern Canada.

These clays are commonly found in the valleys

FIG. 5. - EFFECTIVE STRESS CONDITIONS AT CREEP RUPTURE AND MINIMUM CREEP RATE. (AFTER CAMPANELLA AND VAID, 1972)



of the St. Lawrence and Ottawa Rivers in eastern Canada, as shown in Figure 6.

It's generally agreed that they were deposited in a marine or brackish environment during a brief post - glacial period of isostatic depression and marine invasion. Most of these clays now have a low pore water salt concentration of less than 2g/l which would indicate that much of the salt water has been leached away by perculating fresh ground water.

Recent work by Gadd (1962) suggests that the clay may have first been deposited in a marine environment then the land rose and the clays were redeposited into fresh water. If this were so, some explanation must be found for their open structure and sensitivity. Crawford (1967) proposed that the structure may have been due to flocculation caused by residual cations remaining even after washing by the fresh water.

The sensitive fine - grained sediments of this area are normally called "Leda" clay in engineering literature.

The Leda clays, like other sensitive clays, are thought to have a card house fabric because of their environment during deposition. The stability of such a very open structural arrangement is partly governed by the geometry of the arrangement and partly by the strength of the cohesive bonds at the interparticle contact points. The cohesive bonds are basically due to two

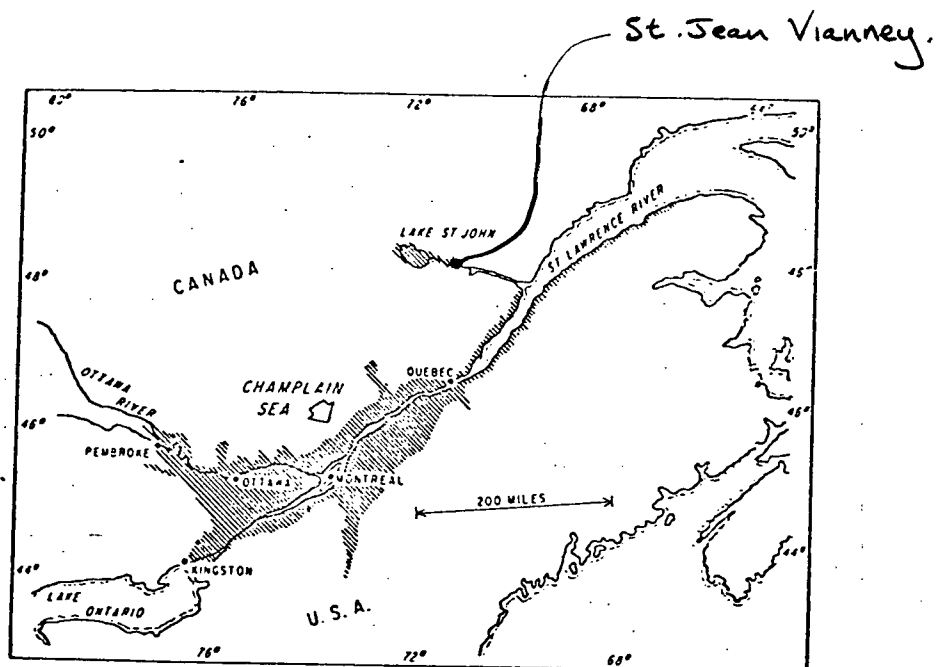


Fig. 6. AREA OF EASTERN CANADA
WHERE LEDA CLAY IS FOUND.

types of bonding, one due to ionic and Van der Waals forces of attraction and the other caused by cementing action of chemical precipitates, mainly ferrous oxides and calcium carbonates. The principle difference between the two types is that during shearing the first type is at least partly redeveloped when new contact points are established, whereas the second type is not. In addition to cohesive bonds a frictional resistance is available at each load bearing contact.

Conlon (1966) and Kenney and Bjerrum (1967) proposed an idea that the combination of the cohesive bonds and the frictional resistance could explain the unusual stress strain curves produced by these quick clays, Figure 7. The mineral skeleton is relatively flexible, so that the deformation is of an elastic nature up to a certain "critical stress", where the maximum resistance of the structural arrangement is reached. At this point bonded contacts between particles begin to fail throughout the structure and its ability to resist shear stresses is greatly reduced, leading to a rearrangement of particles to carry the effective stress and shear forces by sliding resistance. It's only when all effective stresses are transmitted through contact points which are sliding, that the available frictional resistance is fully mobilised. This condition is only reached when the structure is so disturbed and

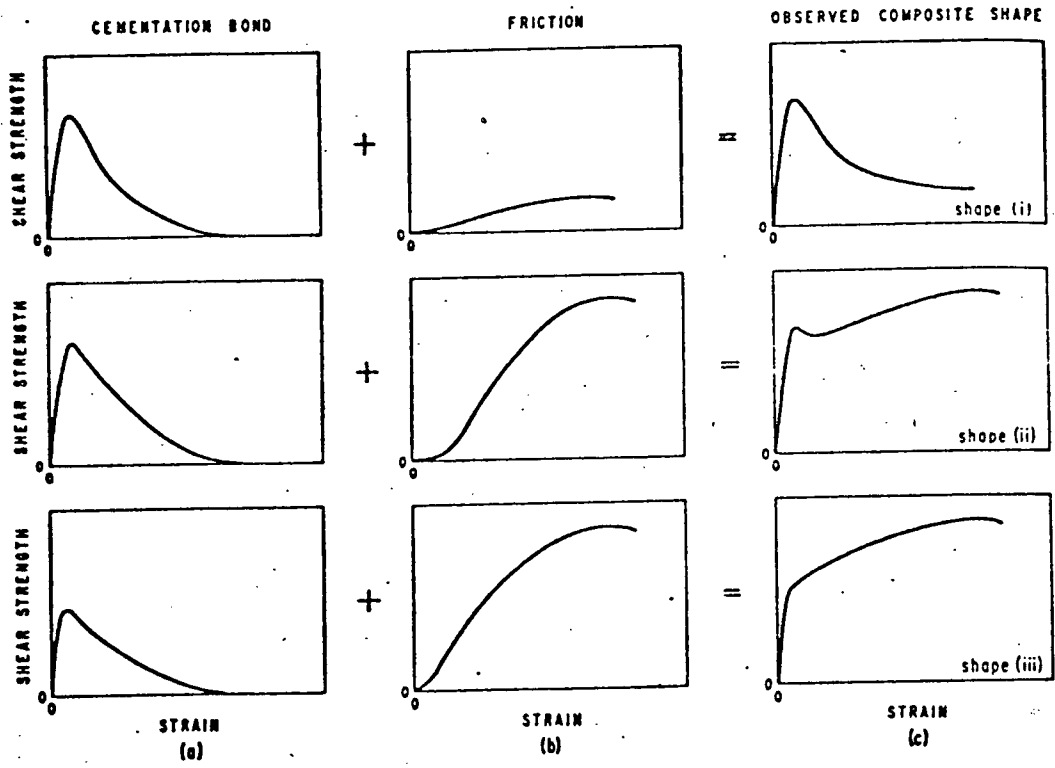


Fig. 7. SCHEMATIC OF THE DEVELOPMENT OF CEMENTATION BOND AND FRICTIONAL STRENGTHS AND THE OBSERVED COMPOSITE SHAPES. (AFTER CONLON, 1966)

the particles so rearranged that all movements are due to sliding of particles over each other in the plane of shearing.

This type of behaviour produces an unusual failure envelope, as illustrated in Figure 8. Below the preconsolidation pressure the peak strength is much higher than the fully mobilised friction envelope. This type of failure envelope makes analysis of stability problems very difficult, especially with natural slopes. Recent investigations, Crawford (1967) and Mitchell (1969), have indicated that effective stress analysis using the method of slices for a first failure gives a reasonable answer, although the influence of the field pore pressure has been found to be of greatest importance. But it is difficult to predict the water conditions in the field. Also the failures are of a progressive nature.

There have been many such failures of natural slopes in eastern Canada, some, such as the slide on the Toulmoustouc River, Quebec in 1962. This was a progressive slide which occurred on a natural slope of only a few degrees. The slide involved 5×10^6 cubic yards of soil. Another major slide occurred in 1971 at Saint - Jean Vianney, Quebec. This slide destroyed 40 homes and killed 31 people. An estimated 9×10^6 cubic yards of material moved during the slide. The slide commenced within the crater of a much larger land slide that occurred about 500 years ago, and after complete

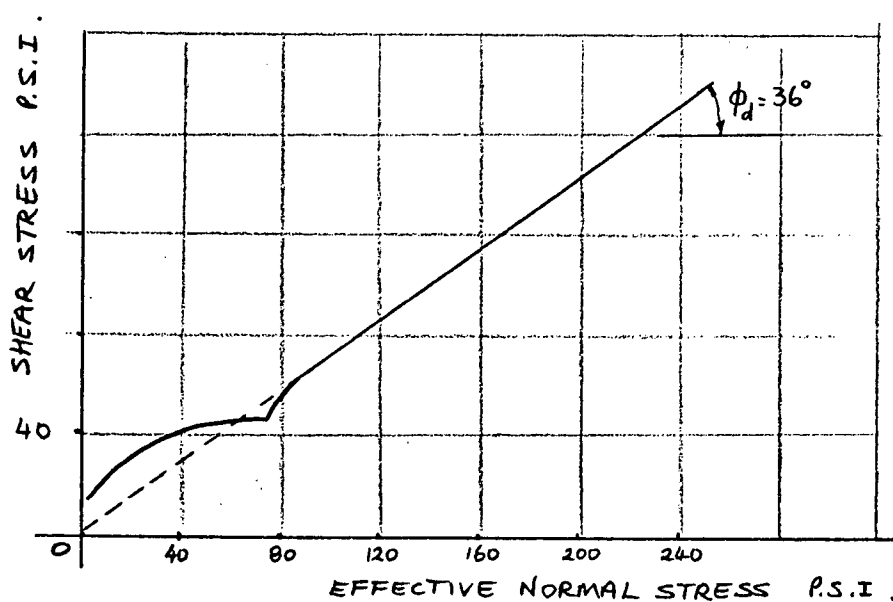


FIG. 8. TYPICAL MOHR-COULOMB PLOT
FOR CONSOLIDATED DRAINED TRIAXIAL
TESTS ON LEDA CLAY. (AFTER CONLON,
1966.)

liquefaction travelled down the Riviere aux Vases at a speed of approximately 16 miles/hour.

Both these slides occurred in May when the water table was at it's highest.

Because of the ridged structure of Leda clays, they have a low index of recompression, but when the load - carrying capacity of the structure is exceeded the compression index is very high. This results in a sharply defined "preconsolidation pressure". Crawford (1967) found that different preconsolidation pressures could be obtained by testing the samples at different rates of loading. Results of these tests are shown in Figure 9.

1.3 Scope

There is an obvious need for more research into these quick clays to obtain a better understanding of their stress - strain relationship, especially with respect to the influence of time.

In this study an attempt has been made to look at the effect of strain rate on the heavily overconsolidation clay from the Saint - Jean - Vianney slide area. All the samples were isotropically consolidated to an all round effective stress of 0.4 Kg/cm^2 . This meant that the samples had an overconsolidation ratio of around 25. Since there are widespread areas where Leda clay deposits are substantially overconsolidated, it was felt that tests in

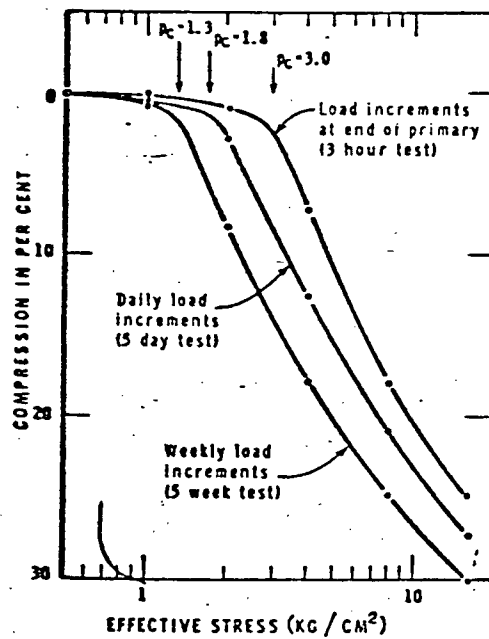


FIG. 9. TYPICAL COMPRESSION-LOG PRESSURE CURVES FOR VARIOUS RATES OF LOADING. (AFTER CRAWFORD,) 1967

this study should be on heavily overconsolidated samples. It was decided to isotropically consolidate the samples because of the ease of using the more conventional equipment and because the results obtained from the creep tests would still produce curves of essentially the same shape as if tested with K_0 consolidation. Also the results were to be studied in a more qualitative rather than quantitative manor.

Undrained strain controlled tests and creep tests were performed along with a group of drained strain controlled tests and creep tests.

The effect of strain rate on the consolidation of Saint - Jean - Vianney clay was also investigated by performing K_0 consolidation tests.

CHAPTER 2

LABORATORY TESTING

2.1 Description of Soil Tested.

The clay used in this testing programme was obtained from the site of the Saint - Jean - Vianney slide in Quebec, and was sampled for Dr. P. LaRochelle of Laval University, Quebec by the Quebec Hydro in June 1971.

The sample was a block sample, 10"x10"x8" high, which had been given many coatings of wax and was stored in a moist room until required.

This clay is normally referred to as Leda clay but in this text will from here after be referred to as S.J.V. clay, after the area from which it came.

This clay was believed to have been deposited in a brackish or marine environment during a brief post - glacial period of isostatic depression and marine invasion. Subsequent leaching by percolating fresh ground water has been one of the reasons for the clays large sensitivity. Cementation at particle contacts has also been postulated as a major cause for the large sensitivity, Crawford (1967) and Kenney (1967). Table 1 shows its typical physical properties.

TABLE 1

PHYSICAL PROPERTIES OF UNDISTURBEDS.J.V. CLAY.

Liquid Limit	36%
Plastic Limit	20%
Plasticity Index	16%
Natural Water Content	42% \pm 1%
Degree of Saturation	100%
Specific Gravity of Solids	2.75
Percent finer than 2 microns	50%
Unconfined compressive Strength	6.5 Kg/cm ²
Sensitivity	around 100
Activity $\frac{P.I.}{\% < 2 \mu}$	0.32
Maximum past pressure	around 10 Kg/cm ²

2.2 Description of the Apparatus.

The main piece of apparatus used in this study was a conventional triaxial cell, in which cylindrical samples 3 inches high by 1.4 inches diameter were isotropically consolidated. A schematic layout of the measuring system is shown in Figure 10. Drainage lines from the top and bottom of the sample were connected to a device which contained a calibrated pipette and differential pressure transducer for measuring volume changes and a pressure transducer for measuring the pore pressure at the base of the sample. The back pressure was applied through the graduated pipette. The cell pressure was applied through a separate plastic water reservoir which also had a pressure transducer attached. Both systems contained a six foot length of $\frac{1}{8}$ " O.D. saran tubing in order to prevent diffusion of air into the system. The vertical deformations were measured by a linear D.C. differential transformer (L.V.D.T.) connected to the loading rod of the triaxial cell. The load was measured by a beryllium copper diaphragm load cell placed above the loading rod.

Signals from all the transducers, load cells and transformers were fed into a Vidar Digital Data Acquisition System. Test data was acquired simultaneously on a magnetic tape and a printer. The Magnetic tape was then used as an input data file while reducing test

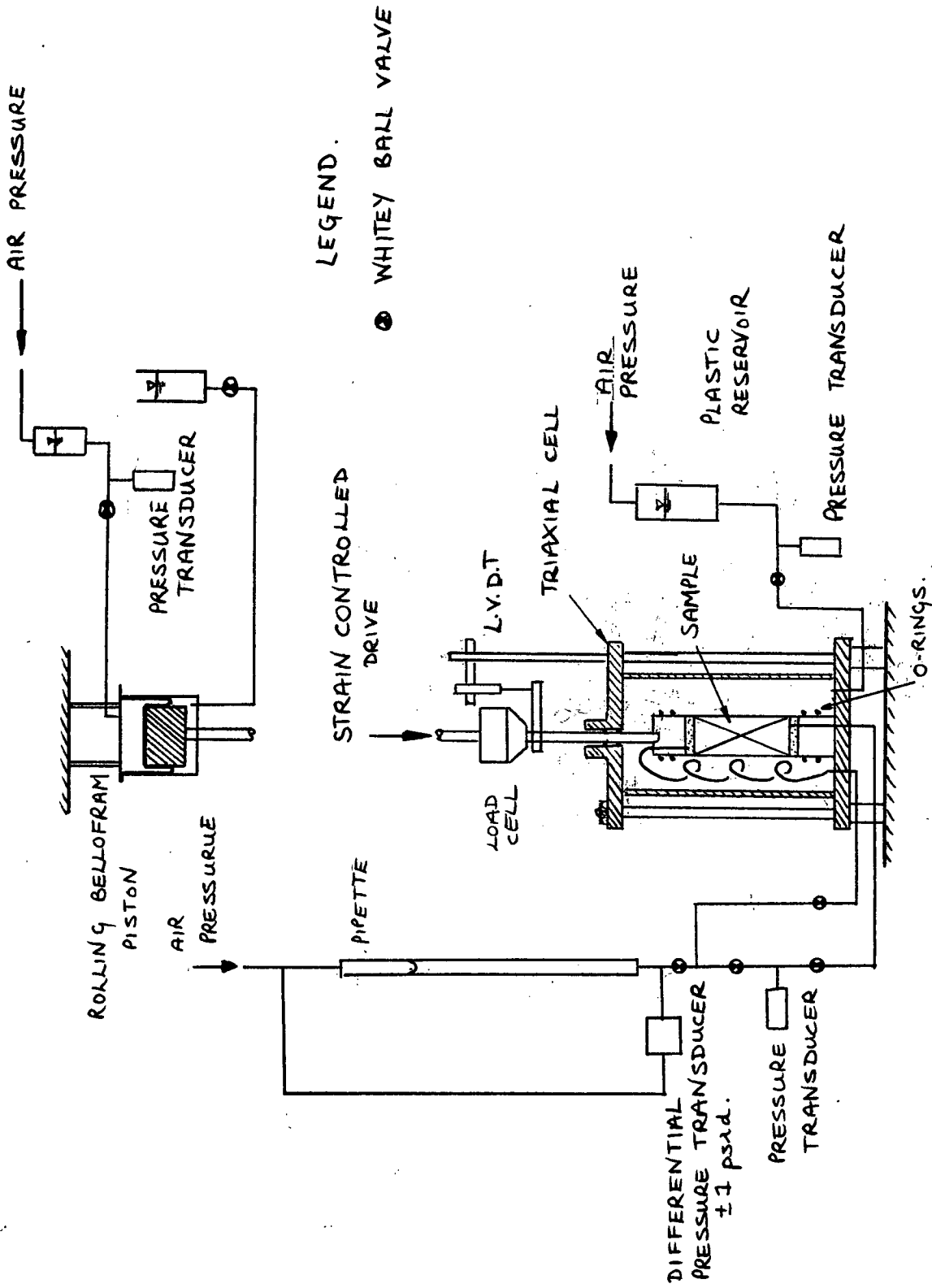


FIG. 10 SCHEMATIC LAYOUT OF LOADING, DISPLACEMENT, PRESSURE AND VOLUME CHANGE MEASURING SYSTEM.

data with the I.B.M. 360/67 computer at U.B.C. Data acquired on the printer helped to keep track of satisfactory progress of the experiments. The high speed automatic recording was particularly useful to enable accurate measurements in the initial and final rupture stages of both the creep and the constant rate of strain tests.

2.3. Experimental Procedure.

Sample Preparation.

Because of the extremely stiff nature of the clay, sample preparation was very difficult. The trimming was done with a sharp knife removing only a small section at a time. The samples were found to contain numerous, very thin, silt lens which had almost zero shear strength in the horizontal direction, such that when the ends of the sample were trimmed there was a tendency for the sample to shear along one of these silt lenses. Thus much care was taken in the trimming of the ends of each sample. It was found that the trimming was aided by preparing the sample in the moist room, this also helped obtain B values nearer to unity.

All the samples were isotropically consolidated for a period of 24 hours, with drainage from both top and bottom of the sample, to an all round effective

stress of approximately 0.4 Kg/cm^2 . Consolidation was done against a back pressure of 3.6 Kg/cm^2 . Normally the sample would have been left undrained for 12 hours to allow any secondary compression to take place, but because the samples were so heavily over consolidated it was felt unnecessary to do this. The first test performed was left, however for 12 hours undrained, after consolidation, but the change in pore pressure was negligible, so it was felt reasonable to omit this step for the remaining tests. All the tests performed were carried out in a constant temperature environment in order to eliminate the influence of temperature as a variable.

Constant Rate of Strain Compression Tests.

For the undrained constant rate of strain compression tests, the valve leading to the pipette was closed after consolidation and the strain rate mechanism started, such that the pore pressure being recorded was from both the top and bottom of the sample, see Figure 10.

For the drained constant rate of strain compression tests, the valve between the pore pressure transducer and the pipette was closed, such that there was drainage from the top of the sample and pore pressure measurements from the base, see Figure 10.

Creep Tests.

The drainage and pore pressure arrangements were the same as for the constant rate of strain tests. The required load was applied through a rolling bellofram piston mounted above the triaxial cell, see Figure 10. The desired level of creep stress was "instantaneously" applied by connecting the loading piston to a preset air pressure through a 3 way valve. As the sample strains under the creep stress, the increase in area causes the stress to decrease slightly, but it was found that the strains encountered were so small very little adjustment was required in order to maintain a constant creep stress.

A summary of all the test information is shown in TableII andIII.

TABLE II

SUMMARY OF TEST INFORMATION FOR STRAIN
CONTROLLED COMPRESSION TESTS

UNDRAINED

TEST NO.	INITIAL W/C %	CONSOLIDATED W/C %	INITIAL HEIGHT (ins.)	VOID RATIO e	MEAN EFFECTIVE CONSOL. STRESS	STRAIN RATE %/min $\dot{\epsilon}$
					$\sigma'_m = \frac{\sigma'_v + 2\sigma'_c}{3}$ Kg/cm ²	
UD1	41.2	41.3	2.976	1.157	0.49	1.6×10^{-3}
UD2	41.4	41.5	2.553	1.161	0.41	2.8×10^{-1}
UD3	41.3	41.4	2.557	1.156	0.40	2.0×10^{-2}
UD4	42.2	42.6	3.121	1.192	0.40	2.8×10^{-1}
UD5	42.1	42.4	3.156	1.186	0.63	7.2×10^{-4}
UD6	42.3	42.6	3.202	1.194	0.40	2.0×10^{-2}

DRAINED

DR.T1	42.4	42.9	3.190	1.201	0.42	7.5×10^{-4}
UD/DR	42.2	42.8	3.170	1.198	0.39	7.5×10^{-4}

TABLE III

SUMMARY OF TEST INFORMATION
FOR THE CREEP TESTS

UNDRAINED

TEST NO.	INITIAL W/C %	CONSOLIDATED W/C %	INITIAL HEIGHT (ins.)	INITIAL VOID RATIO	MEAN EFFECTIVE CONSOL. STRESS	APPLIED STRESS, Kg/cm ² σ_D
					$\sigma'_m = \frac{\sigma'_v + 2\sigma'_c}{3}$ Kg/cm ²	
CR.T1	43.4	44.1	2.745	1.235	0.45	4.71
CR.T2	41.1	42.5	3.146	1.200	0.42	4.32
CR.T3	42.5	44.1	3.041	1.234	0.42	4.22
CR.T4	42.1	42.5	3.199	1.190	0.43	6.30
CR.T5	44.2	45.7	3.231	1.280	0.47	5.97
CR.T6	42.5	43.0	3.268	1.205	0.46	5.74
CR.T6A	43.6	43.9	3.177	1.211	0.49	5.85
CR.T7	43.2	43.8	3.197	1.216	0.43	5.50
CR.T8	42.2	42.8	3.197	1.197	0.45	5.17

DRAINED

DR.CR1	42.2	42.8	2.713	1.197	0.42	4.9
DR.CR2	42.2	42.7	2.918	1.194	0.39	3.8

CHAPTER 3

EFFECTS OF STRAIN RATEON CONSOLIDATION

The consolidation results shown herein were obtained from K_0 consolidation tests performed by Dr. Y. P. Vaid on S. J. V. clay at U. B. C. The tests were performed in a K_0 triaxial cell, details of which have been presented elsewhere, Campanella and Vaid (1972).

The samples were subjected to K_0 one dimensional consolidation under strain controlled loading with drainage permitted from the top and pore pressure recorded at the bottom of the specimen. Four tests were performed at strain rates ranging from 1.13×10^{-5} to 1.95×10^{-7} strain rate/sec. One test was performed using the standard incremental consolidation method.

Figure 11 shows the results of these five tests on a change in void ratio to log vertical effective stress plot. The curves clearly show that the apparent preconsolidation pressure varies from 12Kg/cm^2 for the fastest test to 7.5Kg/cm^2 for the slowest test. The standard incremental method gives an apparent preconsolidation pressure of around 11Kg/cm^2 .

These sharply defined preconsolidation pressures are a clear indication of the sudden breakdown of the rigid structure of S. J. V. Clay. This sudden

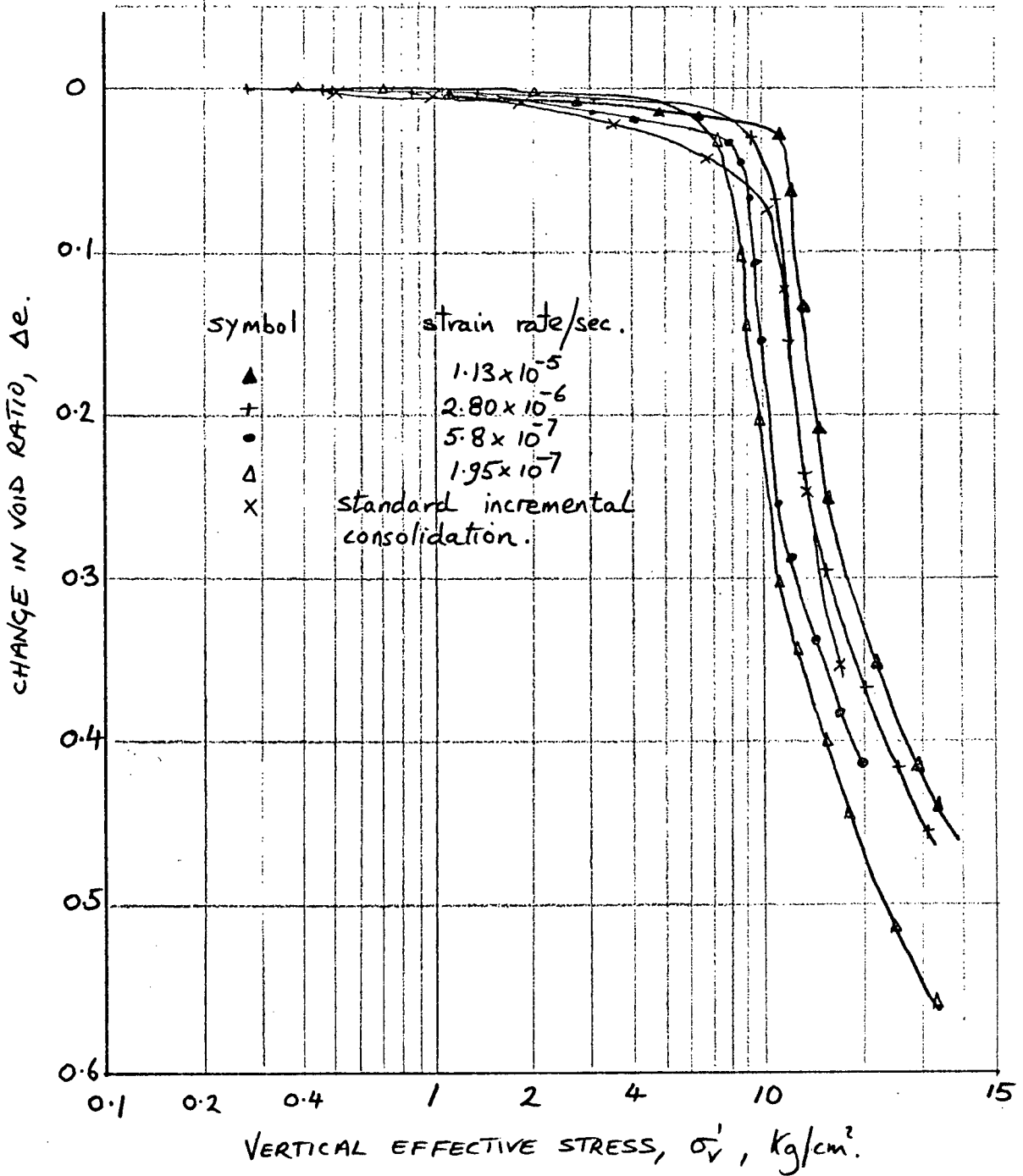


FIG. 11. CHANGE IN VOID RATIO AGAINST VERTICAL EFFECTIVE STRESS FOR K_0 . CONSOLIDATION TESTS ON UNDISTURBED S.J.V. CLAY AT DIFFERENT STRAIN RATES.

breakdown is clearly very strain rate dependant and makes the "correct" preconsolidation pressure extremely difficult to obtained.

Figure 12 shows the change in the coefficient of consolidation, C_v for three of the tests. There appears to be no direct relationship between varying strain rates and C_v , but the range of values was quite large.

The importance of obtaining a valid pre-consolidation pressure is very apparent. If the rate of loading in the field is slow, a standard incremental test could give a very unconservative result. The large range in C_v could also produce a very erroneous estimate for time for consolidation to take place.

Lateral strains were measured throughout the tests and showed that reasonably good K_0 conditions existed for the faster tests, but in the very long tests there was a small amount of leakage leading to lateral strains of around 2.0%.

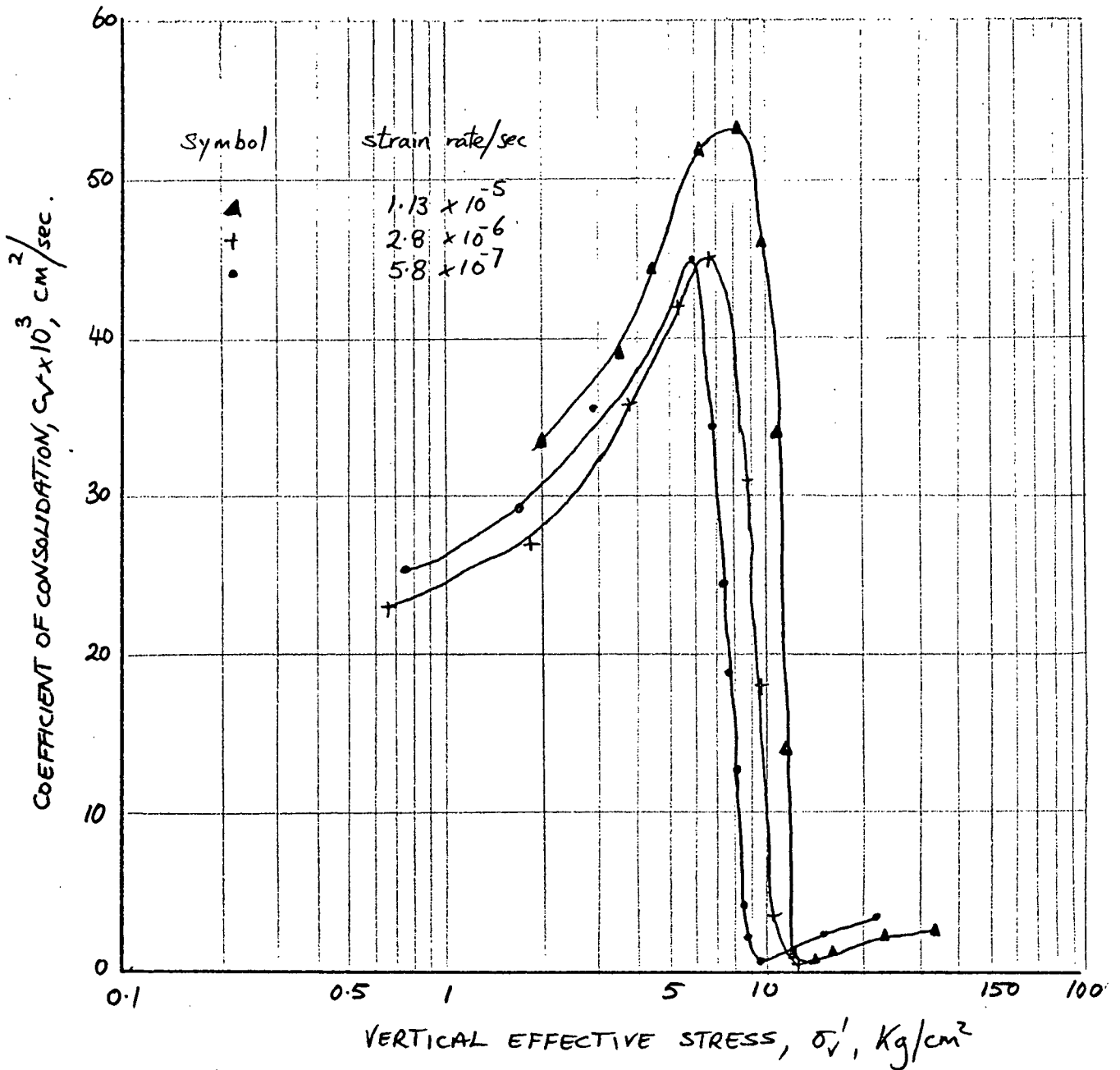


FIG. 12. PLOT OF THE COEFFICIENT OF CONSOLIDATION AGAINST VERTICAL EFFECTIVE STRESS FOR K_0 CONSOLIDATION TESTS ON UNDISTURBED S.J.V. CLAY AT DIFFERENT STRAIN RATES.

CHAPTER 4

RESULTS AND DISCUSSION OF CONSTANT
RATE OF STRAIN COMPRESSION TESTS4.1 UNDRAINED CONSTANT RATE OF STRAIN
COMPRESSION TESTS.

Figures 13 and 14 show the results of the first set of three undrained strain controlled compression tests at different strain rates. Figure 13 clearly shows that there was a 23% increase in deviator stress with over 100 times increase in strain rate. The first part of the curves shows that the distortion was of a linear nature. The effect of strain rate in this linear range before peak deviator stress was quite small in comparison to the point at which peak occurred. It would appear that any bonding that exists within the clay is not very strain rate dependant, except in relation to the point at which the bonds actually break. This point of failure, or peak deviator stress, was reached at between 0.58 and 0.70 percent strain, which is an extremely small strain. This small strain level at peak deviator stress would be expected for such a stiff, over-consolidated and bonded clay.

The strains measured after peak are relatively meaningless because shear was taking place along a single failure surface. This type of failure mechanism

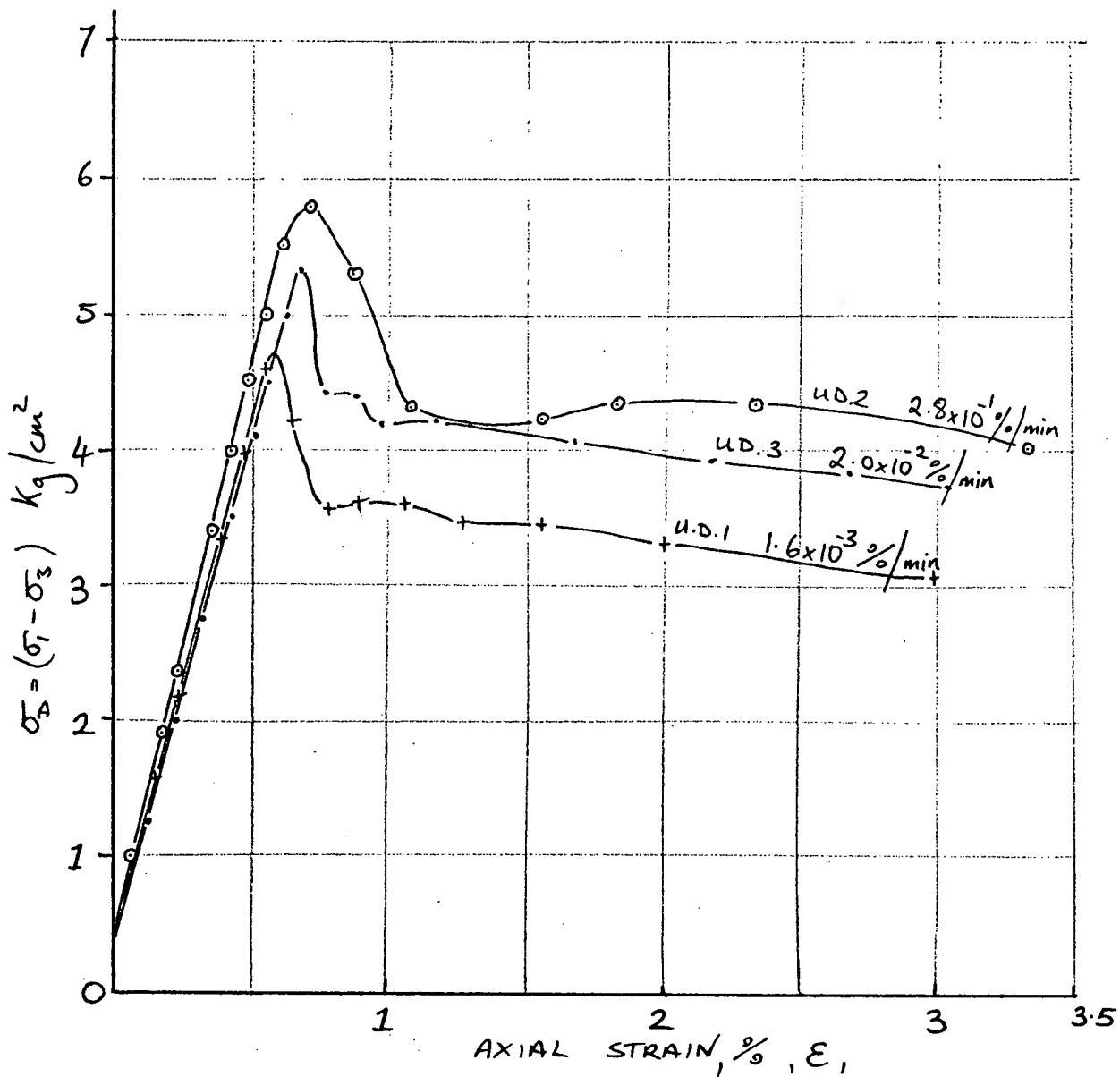


FIG. 13. ISOTROPIC TRIAXIAL CONSTANT RATE OF STRAIN UNDRAINED TESTS ON TOP LAYER OF UNDISTURBED S.S.V. CLAY.

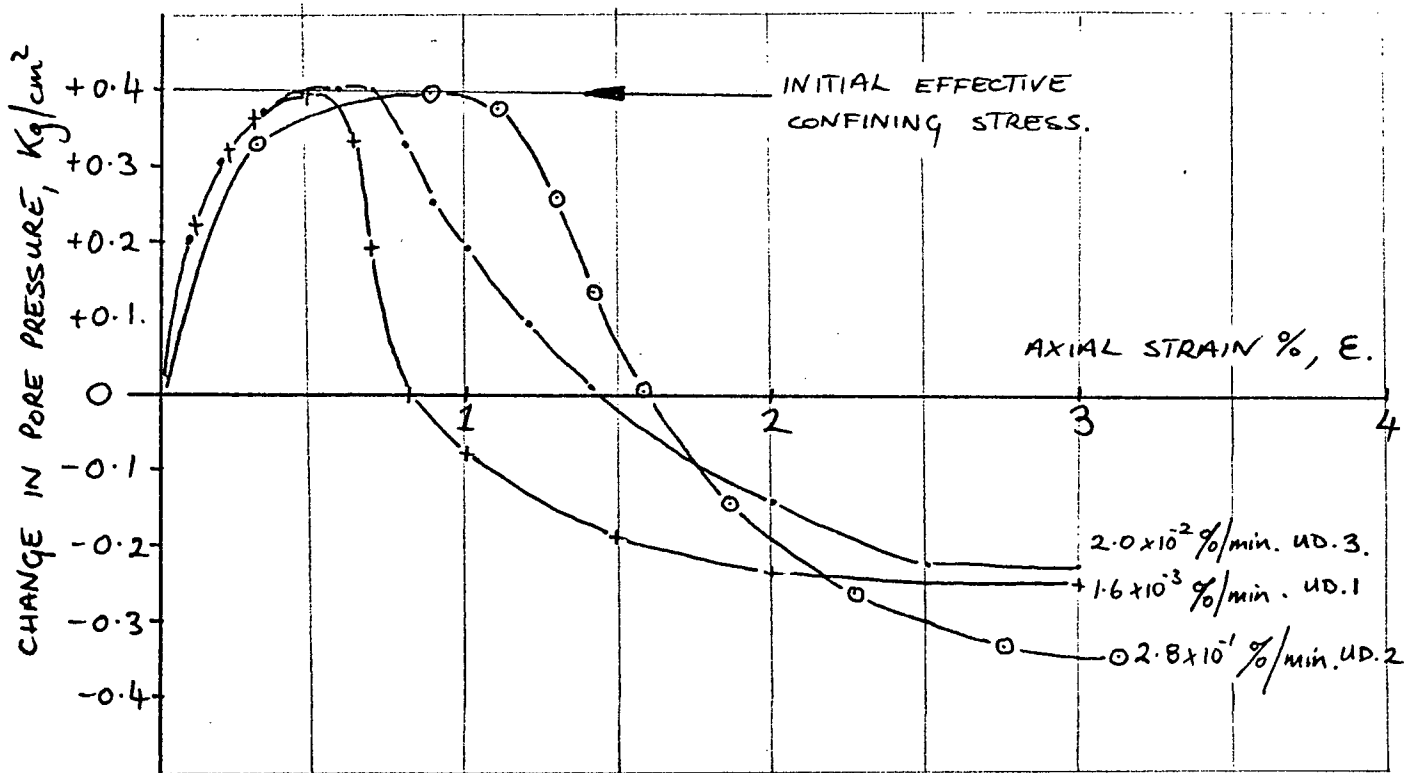


Fig.14. CHANGE IN PORE PRESSURE DURING
 CONSTANT RATE OF STRAIN, UNDRAINED
 COMPRESSION TESTS ON TOP LAYER OF
 UNDISTURBED S.S.V. CLAY.

is to be expected in an overconsolidated clay, since when it is sheared it tends to dilate and so when failure occurs it will appear along a single failure surface.

Figure 14 shows how the pore pressure quickly rose to almost equal the cell pressure then rapidly decrease to a negative value. This rise in pore pressure meant that, at peak deviator stress, the samples were essentially under zero effective confining stress. This resulted in some of the samples showing signs of vertical splitting due to tensile failure, see Appendix II. This also suggests that just about all of the compressive strength of these samples was due to cementation bonding.

The block from which the samples came was so shaped that the samples used for the first three undrained strain controlled compression tests and the first three creep tests were from the top half of the block whilst the remaining samples were from the lower half. Figures 15 and 16 show the results of the undrained strain controlled compression tests on the lower layer of the block, and it can be clearly seen that there was a 28% increase in strength at this second layer to that of the first layer, even though the samples were only inches apart vertically. No complete explanation can be given for this, except that the concentration of silt lenses did appear to be

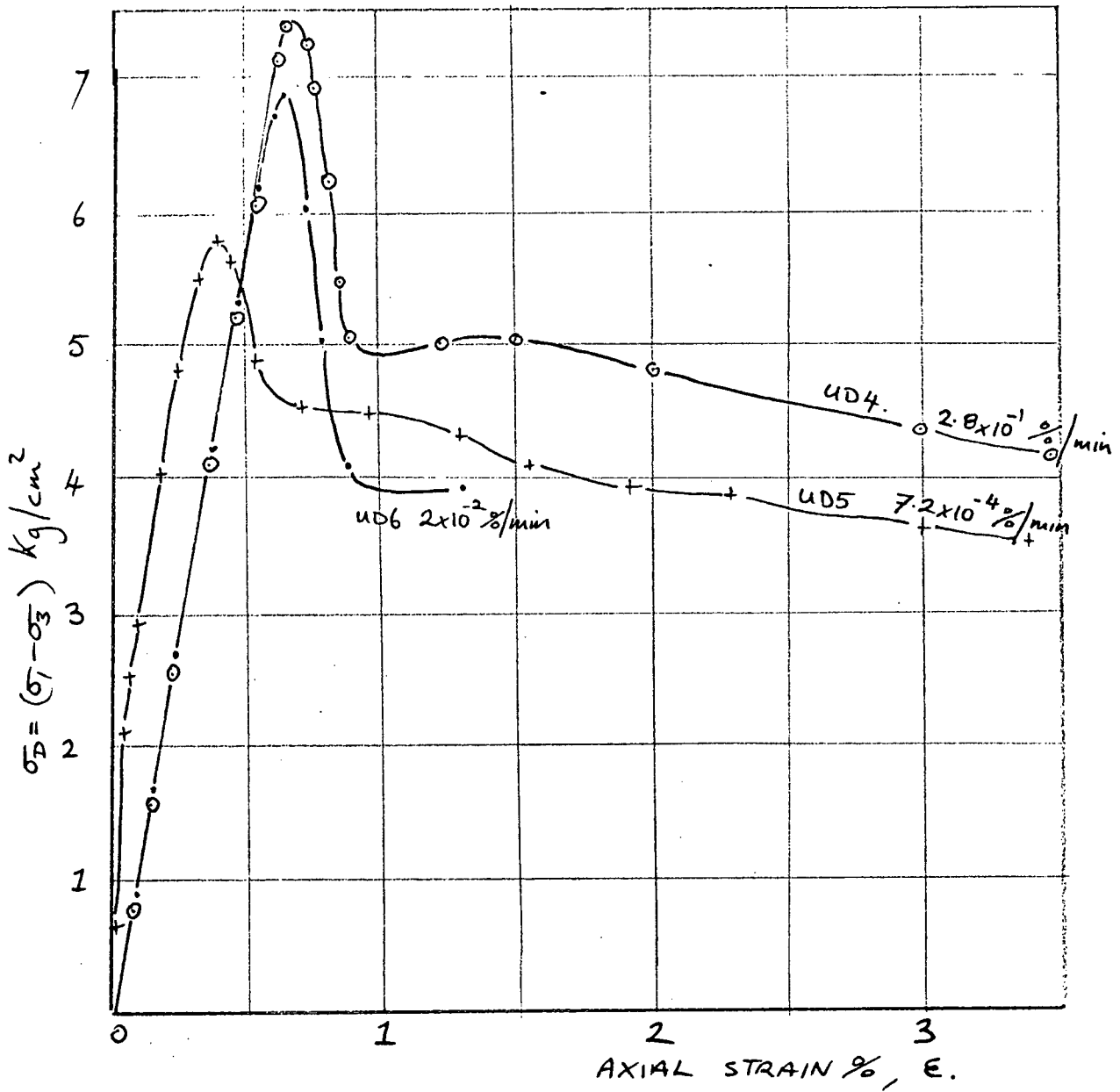


FIG. 15. ISOTROPIC TRIAXIAL CONSTANT RATE OF STRAIN UNDRAINED TESTS ON LOWER LAYER OF UNDISTURBED S.J.V. CLAY.

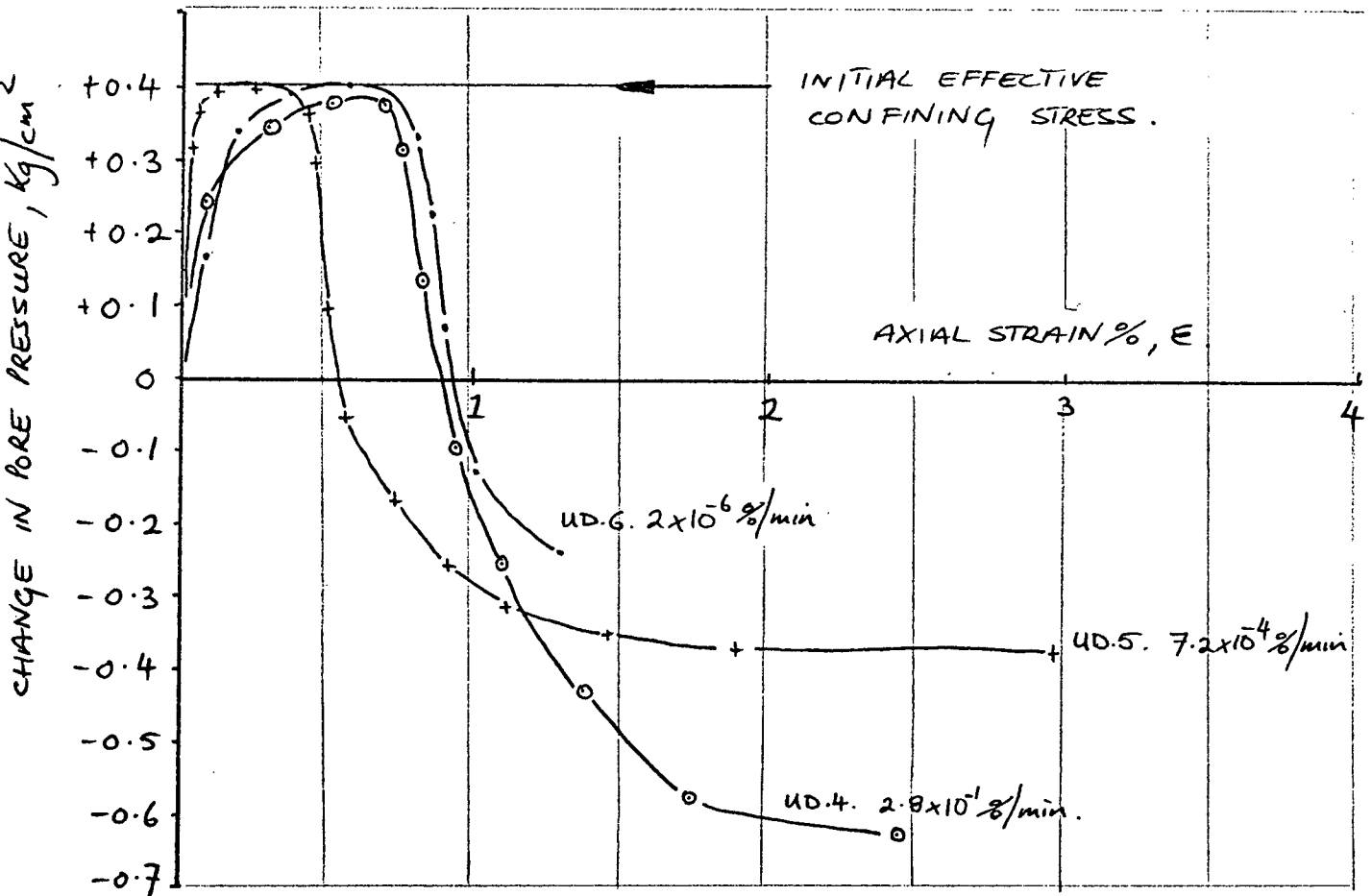


FIG. 16. CHANGE IN PORE PRESSURE DURING
CONSTANT RATE OF STRAIN, UNDRAINED
COMPRESSION TESTS ON LOWER LAYER
OF UNDISTURBED S.J.V. CLAY.

higher in the top layer. Figure 15 also shows that there was still the 25% increase in strength with over 100 times increase in strain rate. The test UD5 appears to be much stiffer prior to peak than the other tests. This could have been just sample variability or more probably due to the unusually large seating load applied during consolidation, see table IV. This extra seating load may have effected the samples initial stiffness but not it's strength, which is dependant on the bonding.

Figure 16 again shows how the pore pressure rose quickly to equal the cell pressure and then after peak dropped rapidly to a negative value. Again this suggest that just about all the strength of these samples was due to cementation bonding and that the bond strength appears to be a function of strain rate.

4.2 DRAINED CONSTANT RATE OF STRAIN COMPRESSION TESTS.

Figures 17 and 18 show the results of the strain controlled drained compression tests, ran at the slowest strain rate. As expected from the results of the undrained compression tests, the reduction in strength after peak was much greater, due to the dilation effects (Swelling) of this heavily overconsolidated clay. Figure 18 shows this dilation effect, where up

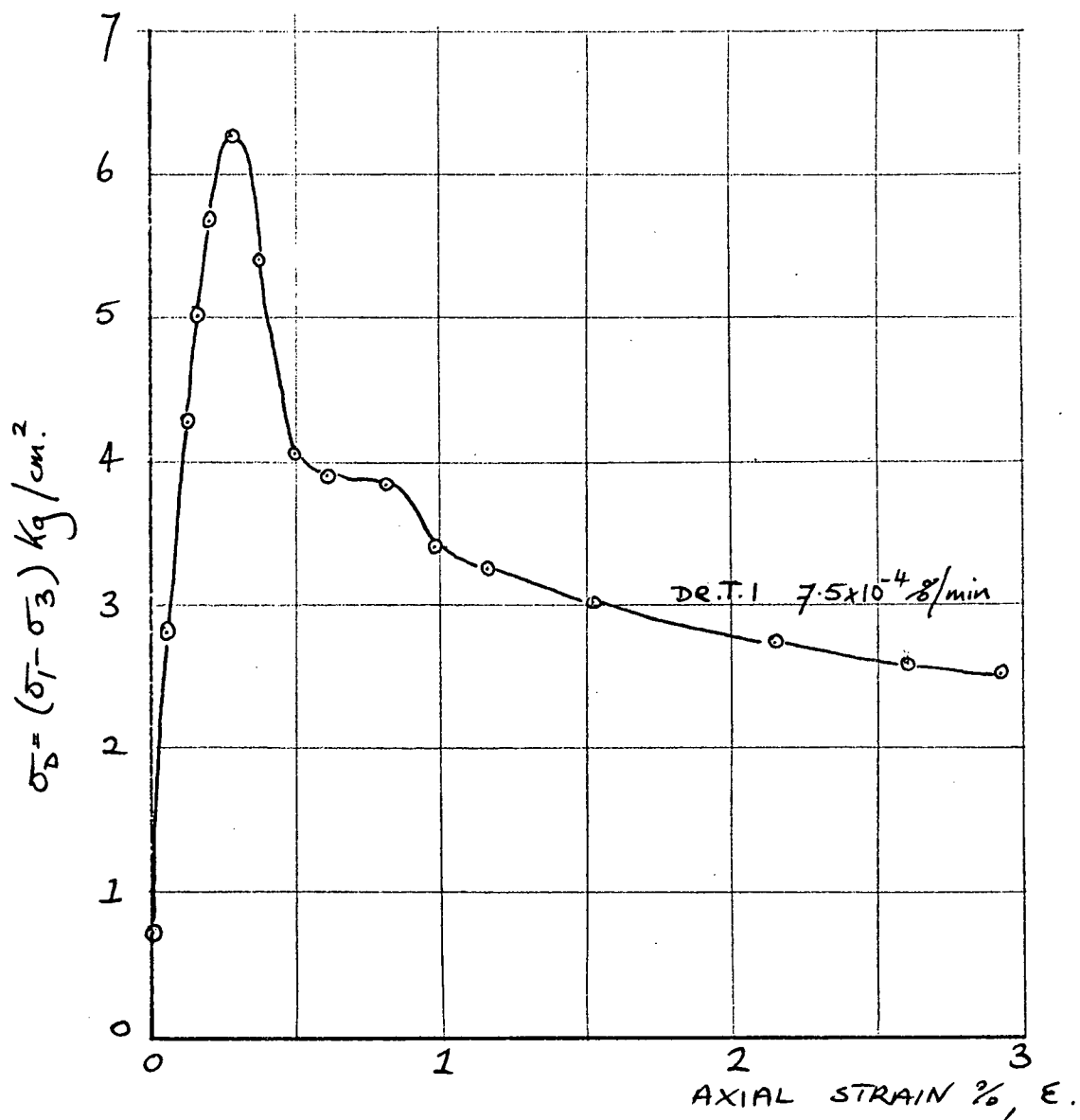


FIG. 17. ISOTROPIC TRIAXIAL CONSTANT RATE OF STRAIN DRAINED TEST ON UNDISTURBED S.J.V. CLAY.

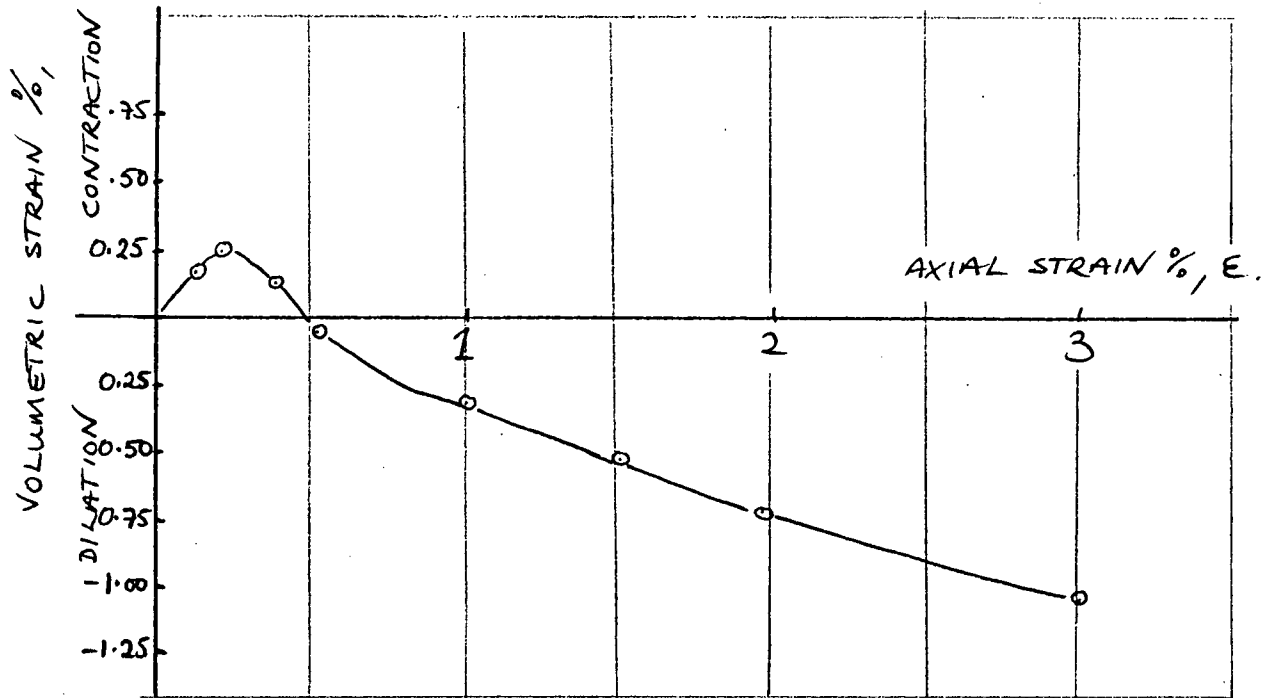


FIG. 18. VOLUMETRIC STRAIN DURING
 CONSTANT RATE OF STRAIN DRAINED
 TEST ON UNDISTURBED S.S.V. CLAY

to peak the sample was contracting slightly, whereas after peak it rapidly dilated.

The failure at peak was so rapid that it was essentially undrained around the failure zone.

After these results it was decided to perform a test where the sample was strained undrained up to its peak and then drainage allowed to occur. The results of this UN/DR. test are shown in Figures 19 and 20. The loss in deviator stress after peak was very marked, more so than the drained test. The results also show that the drained and undrained peak deviator stresses were almost the same but at different strains. Figure 20 shows the variation of pore pressure, measured at the base, plus volumetric strain against axial strain. This plot shows the sharp decrease in pore pressure after drainage was allowed to occur, combined with an initial small decrease in volume followed by a steady increase in volume. Figure 21 shows a comparison of the undrained/drained test with the drained test and one of the undrained test (UD5), all of which were performed at the same level in the block sample. The final strength in the drained condition is clearly much lower than the undrained state due to the increase in water content. Since there is normally water available in the field this large loss in strength could take place after an initial undrained failure.

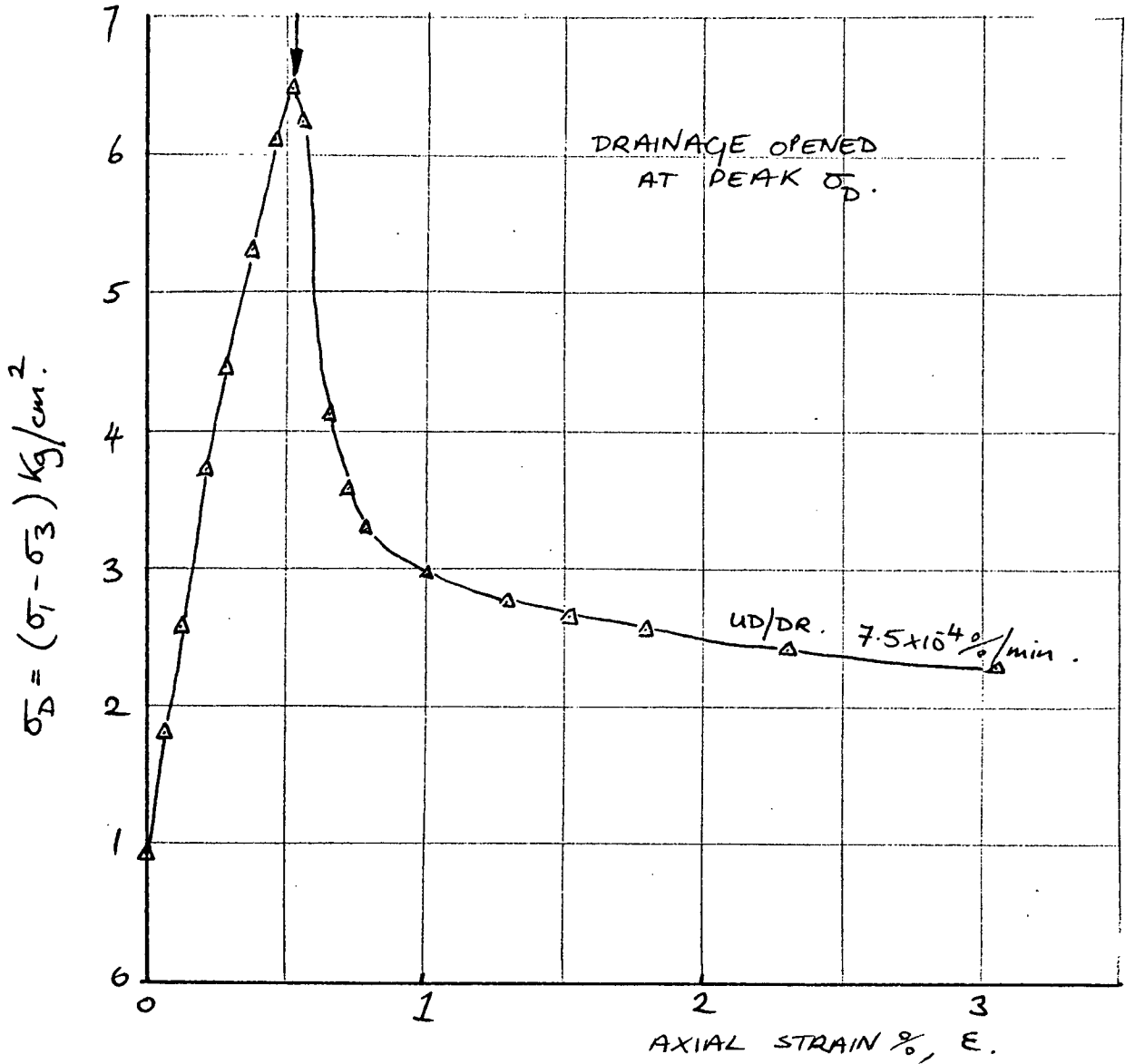


FIG. 19. ISOTROPIC TRIAXIAL CONSTANT RATE OF STRAIN UNDRAINED/DRAINED TEST ON UNDISTURBED S.J.V. CLAY.

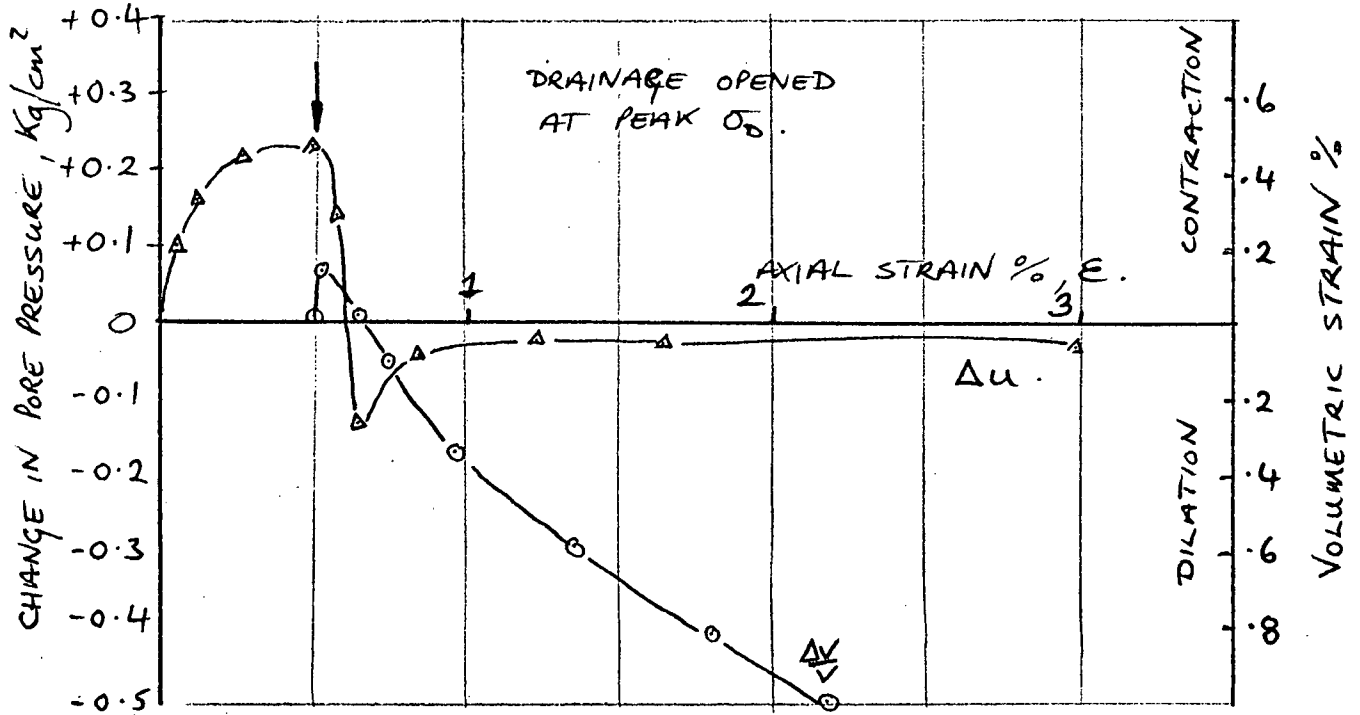


FIG. 20. VOLUMETRIC STRAIN AND CHANGE IN PORE PRESSURE DURING UNDRAINED/DRAINED TEST ON UNDISTURBED S.S.V. CLAY.

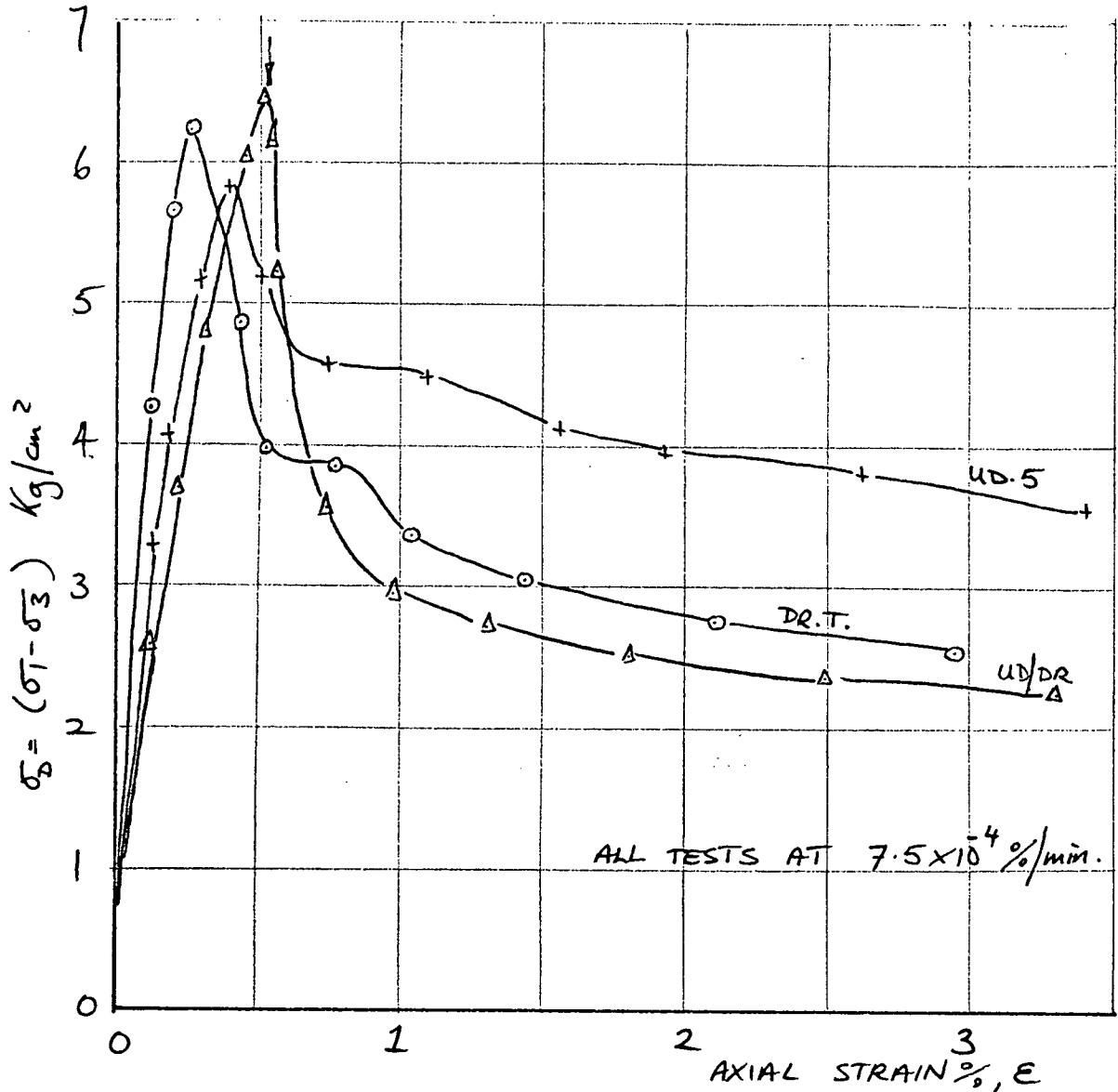


FIG. 21. COMPARISON BETWEEN DRAINED AND UNDRAINED ISOTROPIC TRIAXIAL CONSTANT RATE OF STRAIN TESTS ON UNDISTURBED S.J.V. CLAY.

Figure 22 shows the effective stress path on a modified Mohr plot for one of the undrained strain controlled compression tests (UD2). The stress path shows how the effective stresses within the sample quickly climb and rise up closely to the limit of triaxial testing ($\sigma'_3 = 0$). The stresses continue to rise up closely to this line until peak deviator stress, where upon the stresses drop back sharply. After this sharp drop the stresses begin to climb again and then fall to a lower stress condition. All the undrained strain controlled compression tests followed this same pattern except for the point at which peak deviator stress was reached.

Figure 23 shows the results of all the strain controlled compression tests on the modified Mohr plot. This shows how all the points of peak deviator stress lie on or very close to the limit of triaxial testing, it also shows that the final deviator stress condition lies on a linear envelope passing through the origin that rises at around 33° to the abscissa for a value of $\phi_r = 40^\circ$. This value appears to agree well with the "residual friction envelope" found by Conlon (1966) and shown in Figure 8. Figure 23 implies that the strength of this bonded clay is dependant on effective stresses which is contrary to the concept of a bonded structure. This would indicate that triaxial testing for a bonded

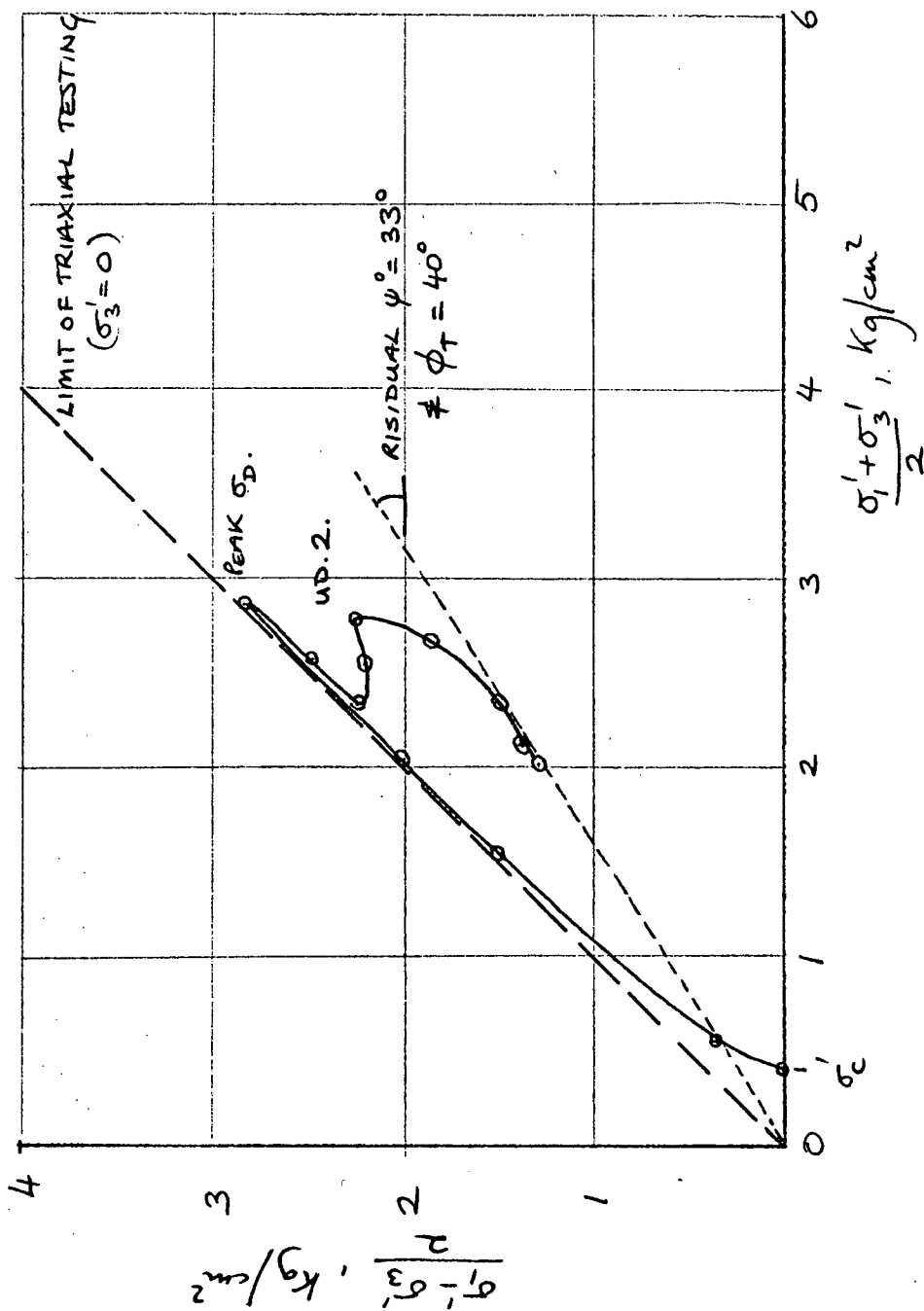
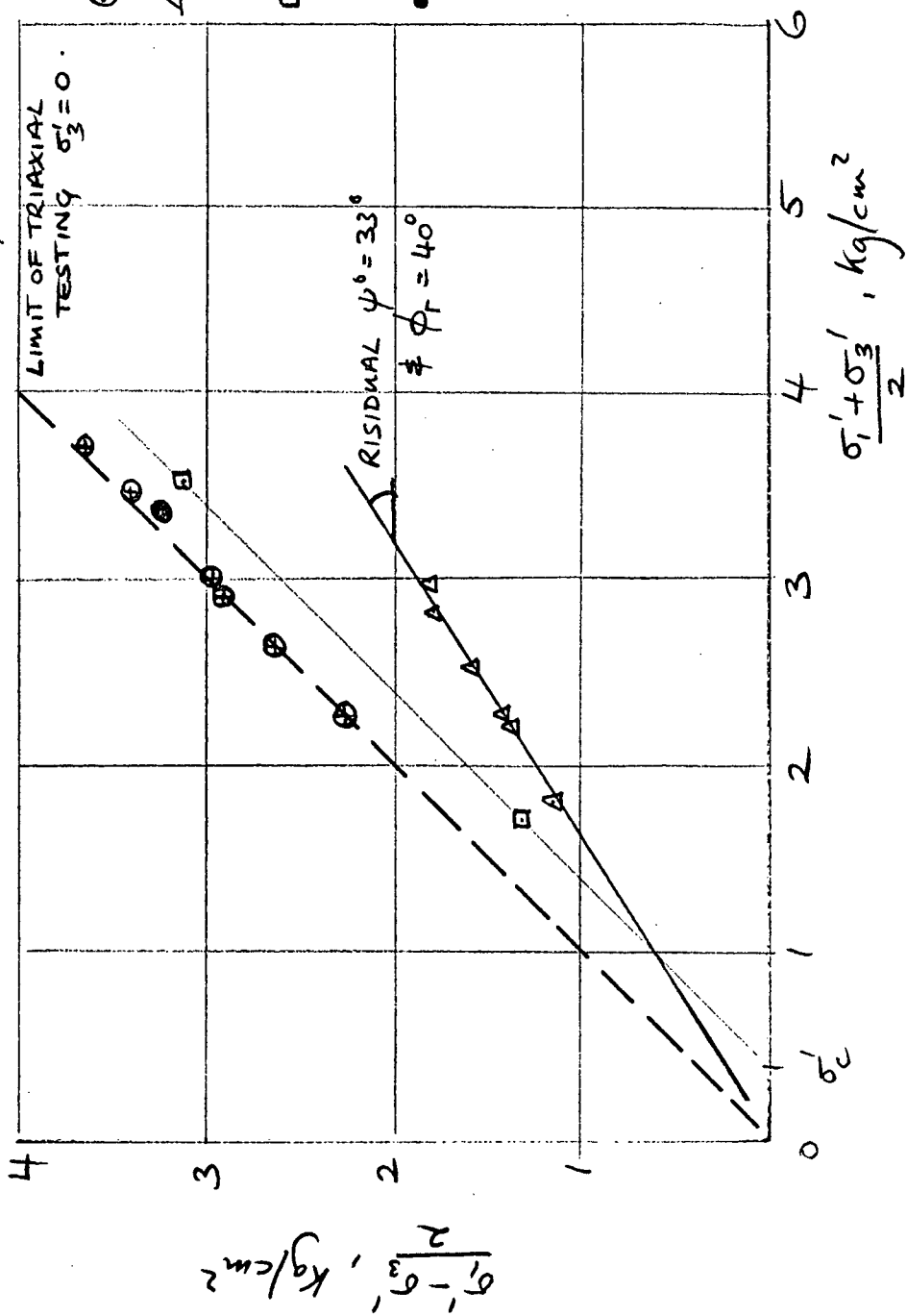


FIG. 22. TYPICAL STRESS PATH FOR STRAIN CONTROLLED UNDRAINED COMPRESSION TESTS.



- ⊕ PEAK DEVIATOR
- △ FINAL DEVIATOR (STRAIN > 3%)
- DRAINED STRAIN CONTROLLED TEST
- UNDRAINED/DRAINED STRAIN CONTROLLED TEST.

FIG. 23. EFFECTIVE STRESS CONDITION FOR STRAIN CONTROLLED COMPRESSION TESTS AT PEAK AND FINAL DEVIATOR STRESS.

clay at such a low stress level is ineffective in obtaining the complete failure envelope.

Also plotted on Figure 23 are the peak and final deviator stress conditions for the drained test. These points lie on a line that rises at 45° from the initial stress condition, which would be expected for a drained test. The final deviator stress condition lies very close to the residual friction envelope produced from the undrained tests.

A summary of all the results for the strain controlled compression tests is shown in table IV. This table shows that the peak deviator stress, σ_d , was reached at strains ranging from 0.40 to 0.70% for the undrained tests, and 0.26% for the drained test. These very small strains were reached in times ranging from $5\frac{1}{2}$ minutes to 860 minutes for the undrained tests and 961 minutes for the drained test. The pore pressure parameter at failure, A_f , for the undrained tests, were all around -0.5, which was as expected for an over-consolidated clay.

TABLE IV

SUMMARY OF RESULTS OF STRAIN
CONTROLLED COMPRESSION TESTS.

UNDRAINED

TEST No.	STRAIN RATE $\dot{\epsilon}$ %/min	PEAK σ_p Kg/cm ²	FINAL σ_p ($>3\%$) ₂ Kg/cm ²	STRAIN AT PEAK σ_p %/min	TIME TO PEAK MINS	PORE PRESSURE PARAMETER AT PEAK σ_p . Af.
UD1	1.6×10^{-3}	4.70	3.10	0.58	420	-0.74
UD2	2.8×10^{-1}	5.80	4.20	0.70	5.5	-0.56
UD3	2.0×10^{-2}	5.35	3.75	0.68	57	-0.55
UD4	2.8×10^{-1}	7.45	4.40	0.68	6.7	-0.60
UD5	7.2×10^{-4}	5.80	3.60	0.40	860	-0.54
UD6	2.0×10^{-2}	6.90	N/A	0.65	54	-0.58

DRAINED

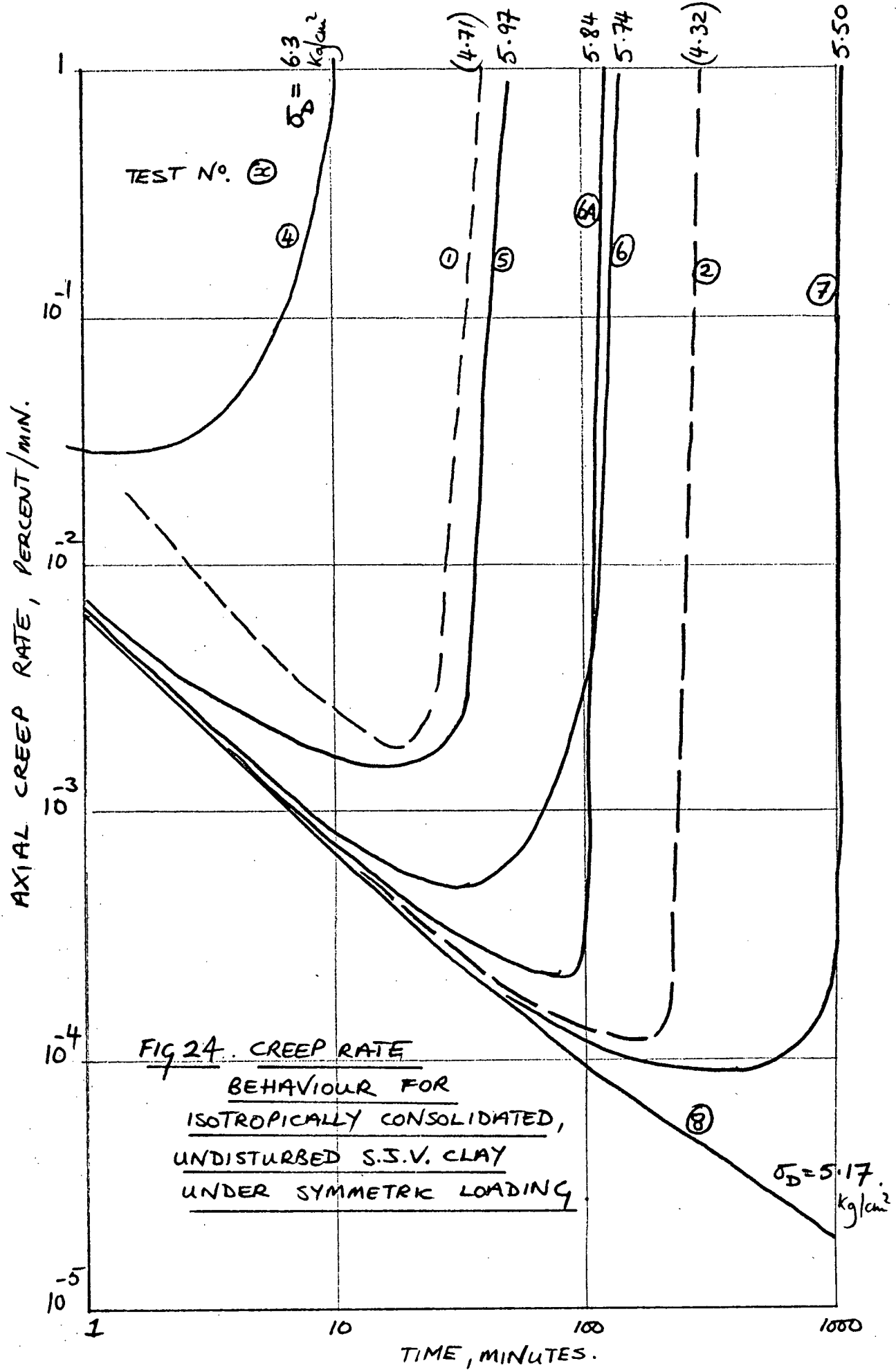
TEST No.	STRAIN RATE $\dot{\epsilon}$ %/min	PEAK σ_p Kg/cm ²	FINAL σ_p ($>3\%$) ₂ Kg/cm ²	STRAIN AT PEAK σ_p %/min	TIME TO PEAK MINS	VOLUME CHANGE cm ³
DR.T	7.5×10^{-4}	6.25	2.55	0.26	961	0.26
UD/DR	7.5×10^{-4}	6.50	2.30	0.52	945	N/A

CHAPTER 5

RESULTS AND DISCUSSION OF CREEP TESTS.5.1 UNDRAINED CREEP TESTS

Figure 24 is a plot of axial creep rate against time, in minutes, and shows that initially the creep rate is very fast, but with time decreases to a minimum, where upon it begins to increase rapidly again, leading to failure. These curves differ from those found by Snead (1970) and Campanella and Vaid (1972), in that initially all the tests follow more closely the same line of decreasing creep rate. This agrees well with the reaction obtained from the strain controlled compression tests prior to peak, since they all tended to follow the same stress-strain line. Results of all the creep tests have been plotted on Figure 24. It is interesting to see that even though the samples tested from the top layer of the block (CR.T.1,2 and 3), which had lower strengths, still lie along the same initially decreasing creep rate line.

Results from Figure 24 suggest that the onset of an accelerating creep rate indicates impending failure, since as long as the creep rate is increasing, failure is inevitable. However, sufficient warning concerning rupture was usually present, since elapsed time until rupture (rupture life) was generally around



twice the elapsed time up to the point when the creep rate started accelerating (minimum creep rate).

Figure 25 shows the rupture life, t_r , for each stress level plotted against the corresponding minimum creep rate, $\dot{\epsilon}_{\min}$, on a log-log scale. This plot shows that there exists a reasonable straight line relationship between the rupture life and the minimum creep rate, regardless of stress level. In long term tests, the rupture life could be estimated from this relationship as soon as the minimum creep rate has occurred. Unfortunately the width of error bands are extremely large, which shows that for a given minimum creep rate, rupture life could vary by as much as a factor of 5.

Since, for natural slopes in the field, the start of creep is not usually known, a plot of minimum creep rate against remaining time to rupture is shown in Figure 26, for all the creep tests. Again a reasonable straight linear relationship is shown with the same error band as Figure 25. This relationship would indicate that once the minimum creep rate has been reached, and its value found, an estimate of the remaining time to rupture can be obtained. But again, since it would be difficult to obtain the point of minimum creep rate in the field, a plot of tertiary, or accelerating creep rate against remaining time to rupture, tt_r , has been

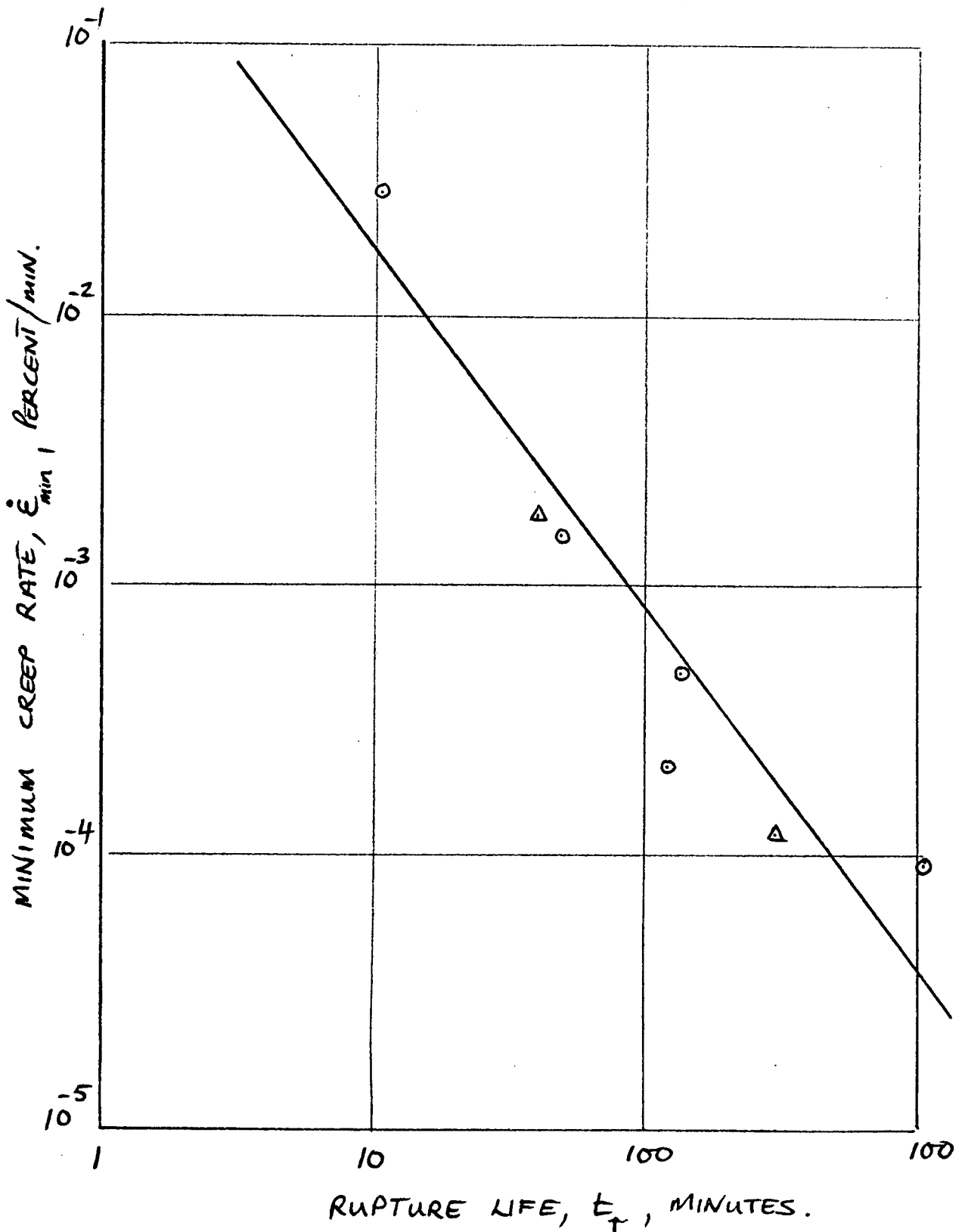


FIG. 25. RELATIONSHIP BETWEEN RUPTURE LIFE AND MINIMUM CREEP RATE FOR ISOTROPICALLY CONSOLIDATED UNDISTURBED S.S.V. CLAY.

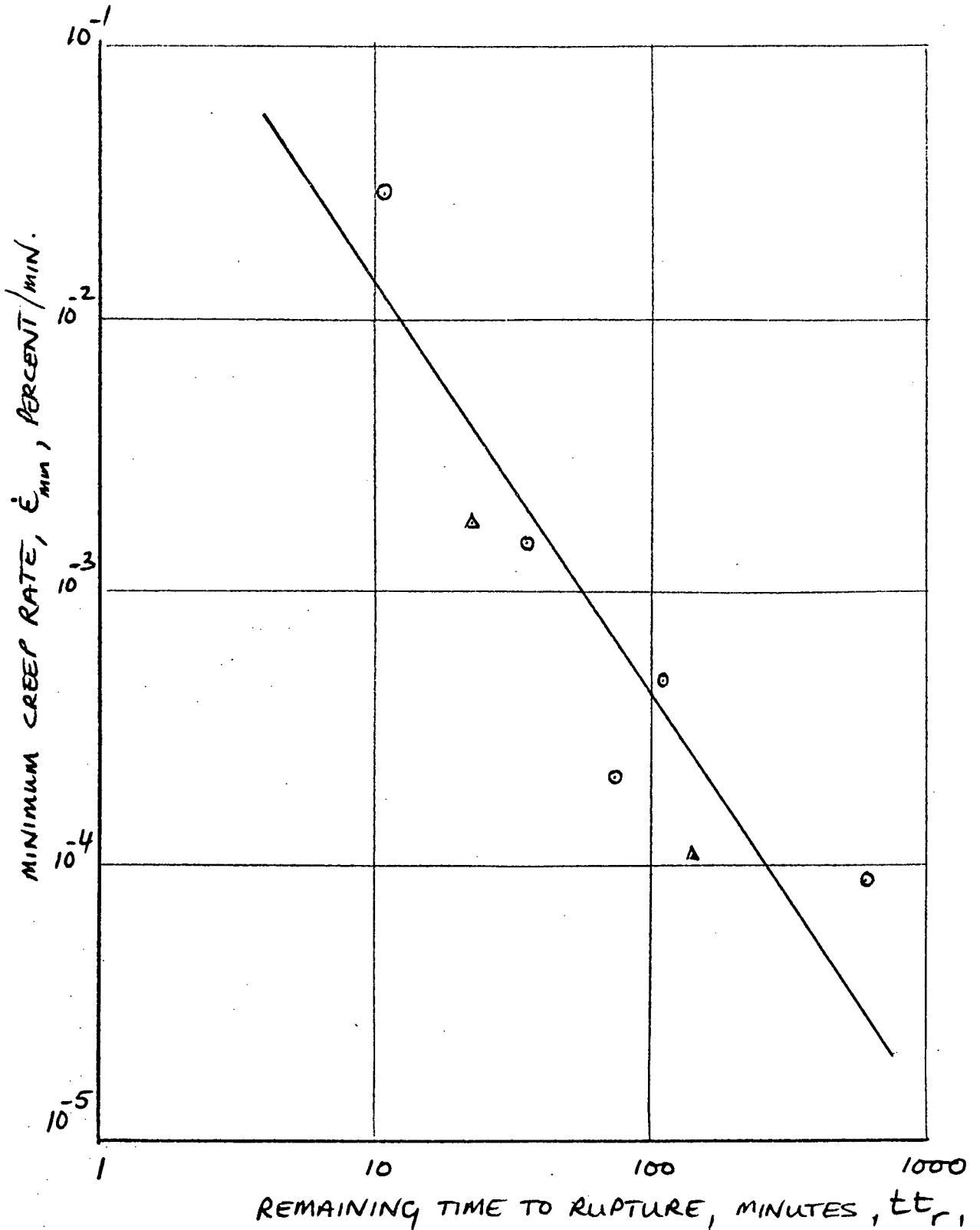


FIG. 26. RELATIONSHIP BETWEEN MINIMUM CREEP RATE AND REMAINING TIME TO RUPTURE FOR ISOTROPICALLY CONSOLIDATED UNDISTURBED S.J.V. CLAY

plotted in Figure 27, for three of the creep tests. The scatter of the points was extremely large when all the tests were plotted, so the data was separated into its individual tests and separate lines plotted for each, of which only three are shown in Figure 27. Campanella and Vaid (1972) obtained a single line for all their tests at different stress levels, unlike the separate lines obtained here. Part of the reason for this disagreement could be due to the difficulty of obtaining reasonable data for this quick clay in the tertiary creep rate range, also the fact that strains measured near to rupture are meaningless due to the movement along a single failure plane.

It was apparent from Figure 24 that as the creep stress level increased the rupture life progressively decreased. Figure 28 shows the relationship between creep stress and the corresponding minimum creep rate for both layers of the block sample. Both lines appear to be parallel although the data available for the top layer was obviously limited. Figure 29 shows the same plot, but with the stress levels at peak deviator stress plotted for all the undrained strain controlled compression tests, the dotted lines on the plot are the creep data as from Figure 28. Although the data is a little scattered there does appear to be a trend that would indicate the existence of a possible

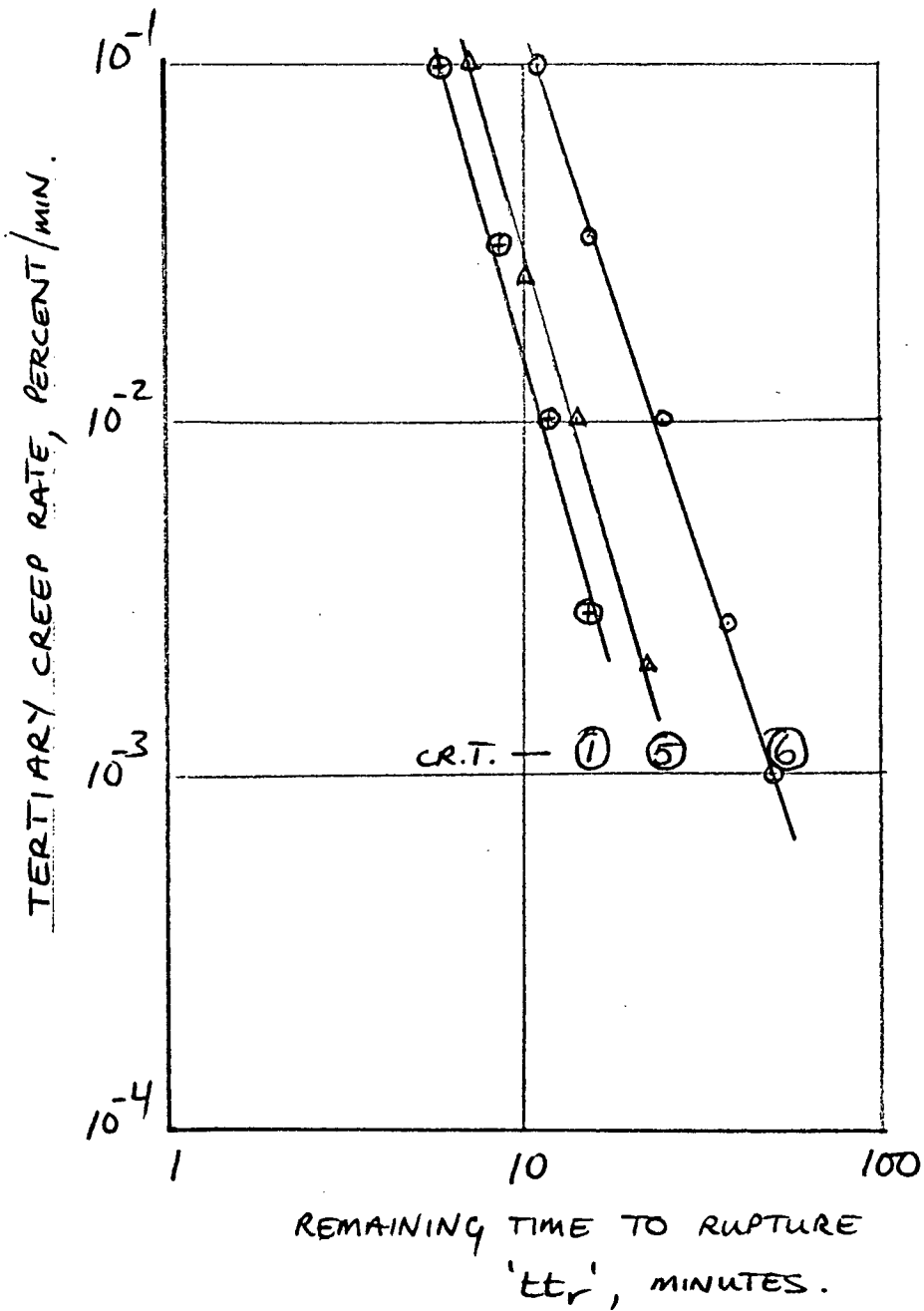


Fig. 27. SOME TYPICAL CURVES FOR TERTIARY CREEP RATE AGAINST REMAINING TIME TO RUPTURE, t_{tr} , FOR ISOTROPICALLY CONSOLIDATED UNDISTURBED S.S.V. CLAY.

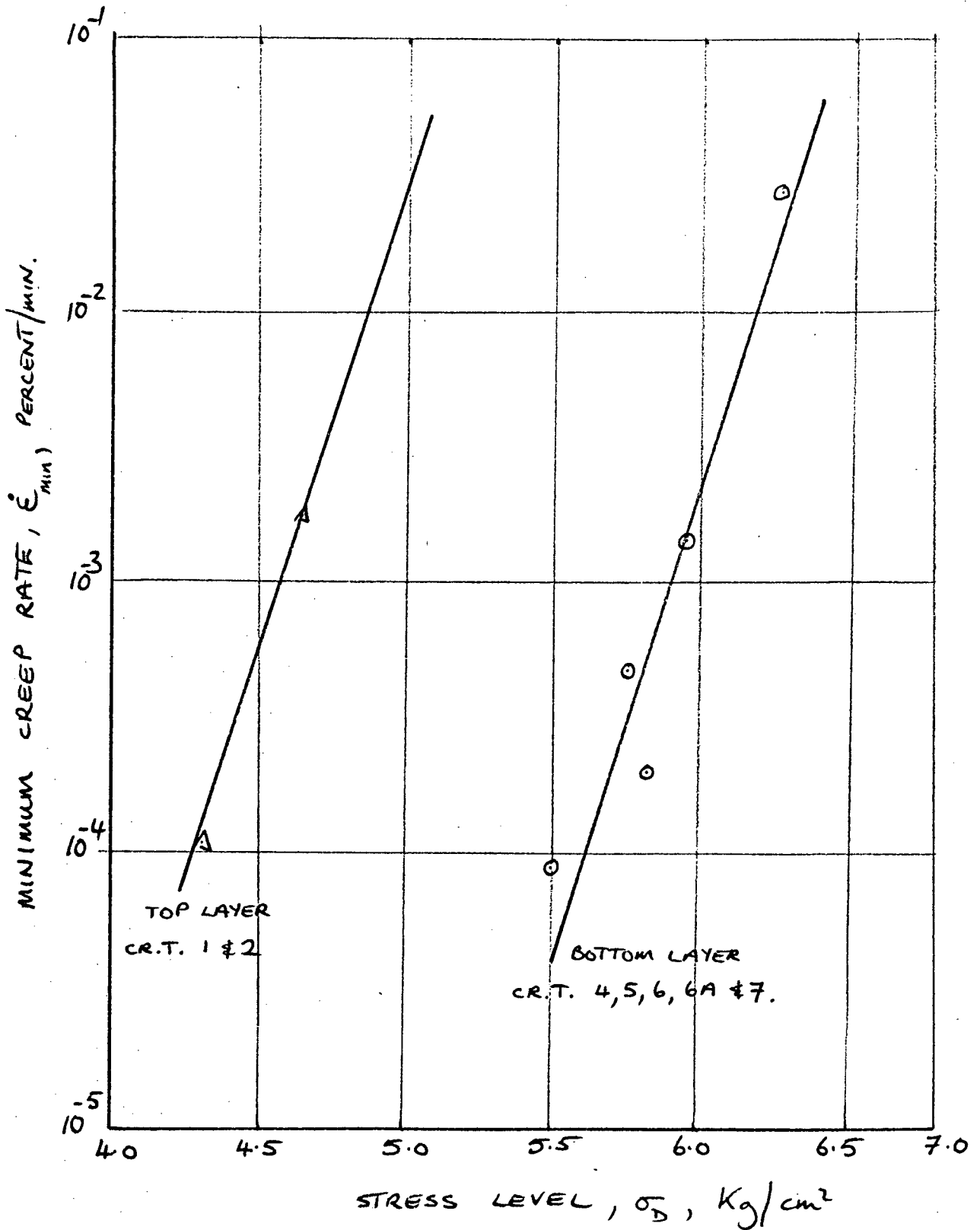


Fig. 28. RELATIONSHIP BETWEEN MINIMUM CREEP RATE AND STRESS LEVEL FOR BOTH LAYERS OF THE BLOCK SAMPLE OF S.J.V. CLAY.

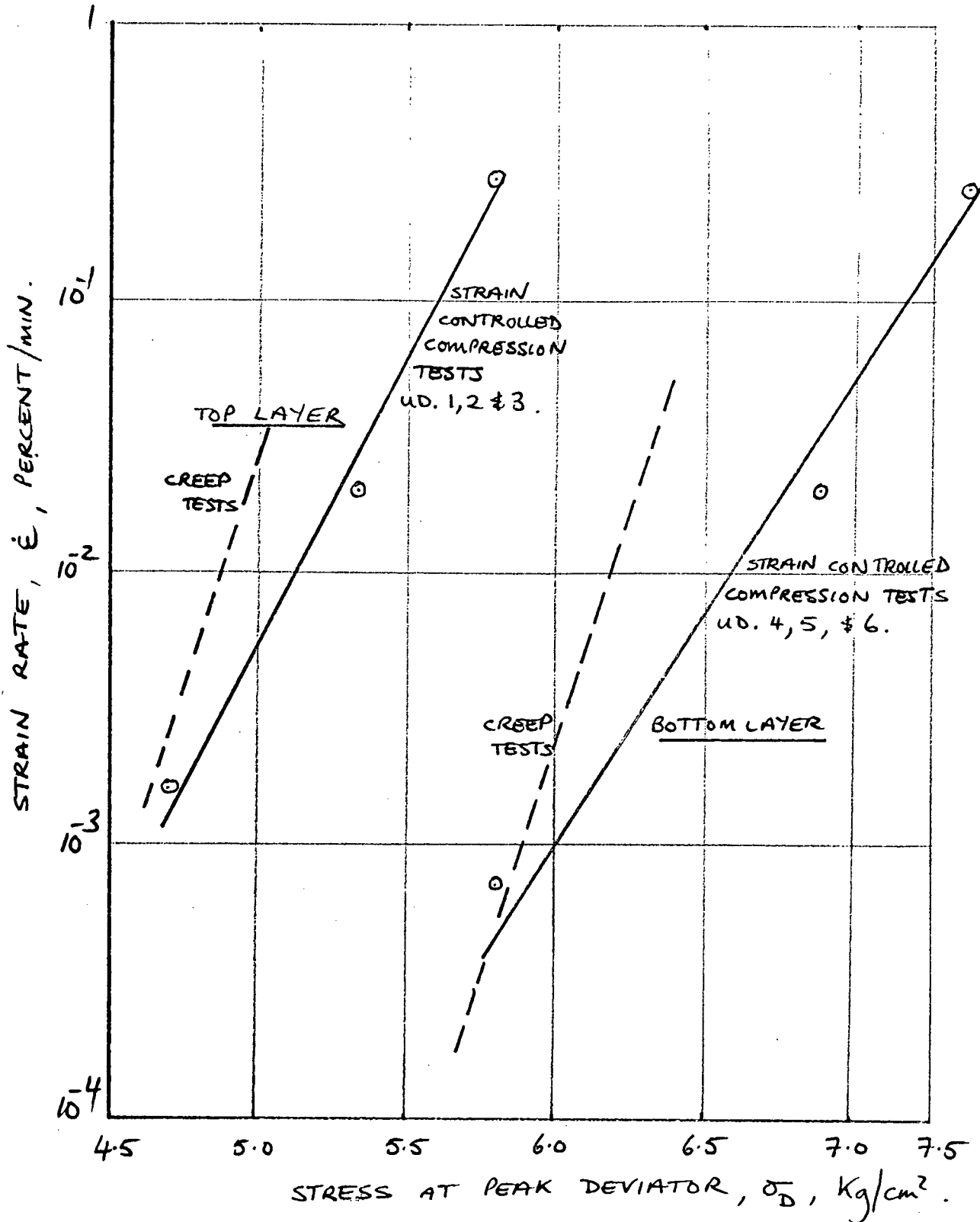


FIG. 29. RELATIONSHIP BETWEEN PEAK DEVIATOR STRESS AND STRAIN RATE FOR UNDRAINED STRAIN CONTROLLED TESTS ON BOTH LAYERS OF THE BLOCK SAMPLE OF S.J.V. CLAY.

relationship between strain rate and stress regardless of the testing method.

Figure 30 shows a plot of stress level against log time to rupture for the creep tests performed on the bottom layer of the block sample. At higher stress levels the creep strength shows essentially a linear decrease with log rupture life. At lower stress levels, however, the decrease in creep strength was much slower with time to rupture and the form of the curve seems to indicate the existence of a long term yield strength below which creep rupture will not occur. This is usually termed the upper yield strength.

There are various methods of estimating the upper yield strength from creep test results, but because of the limited number of tests performed here, no realistic value can be obtained. These methods require a large number of tests to be performed, which is not always possible, but if two strain controlled compression tests are performed at different, very slow strain rates and give the same strength, then that strength can be regarded as the upper yield strength.

5.2 DRAINED CREEP TESTS.

One drained creep test was performed, DR.CR1, but due to the problems with the availability of the Vidar Digital Data Acquisition very little

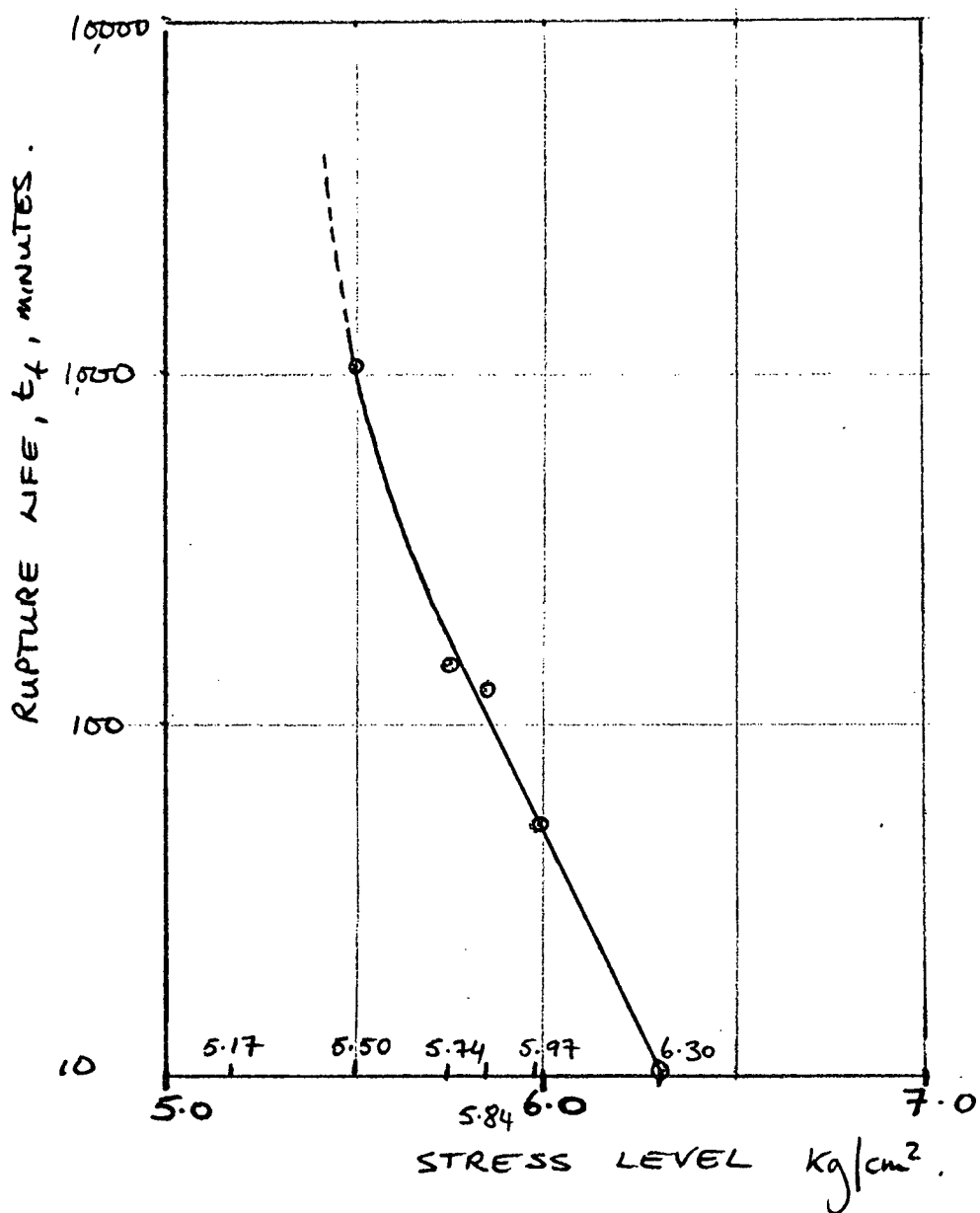


FIG. 30. VARIATION OF CREEP STRENGTH WITH TIME TO RUPTURE FOR ISOTROPICALLY CONSOLIDATED S.S.V. CLAY.

information was obtained to fully analysis the results. Figure 31 shows a plot of axial strain rate against time, and the curve for DR.CR1 is shown, as plotted from the available data. It can be seen from Figure 31 that the curve for this drained test followed very much the same pattern as the undrained tests.

Another drained test was performed, DR.CR2, in which the applied stress level was much lower than that applied in DR.CR1. It is interesting to see that the curve at the lower stress level plots above that of the higher stress level curve, which is contrary to the undrained creep curves. After 3000 minutes of loading for DR.CR2, the pore pressure was boosted by 0.1 Kg/cm^2 to try and simulate a rise in the watertable in natural slopes. It can be seen from Figure 31 that this increase in pore pressure caused an immediate increase in strain rate, which after a period of time reached a maximum and then began to decrease again. This continued for another 3000 minutes where the pore pressure was again boosted by 0.1 Kg/cm^2 , but again, due to problems with the availability of the Vidar and also the fact that the strain measured remained practically constant, the curve has been terminated. The test was, however, kept running for another 3000 minutes, in which time it was observed that the strain remained almost constant but the sample was sucking in water.

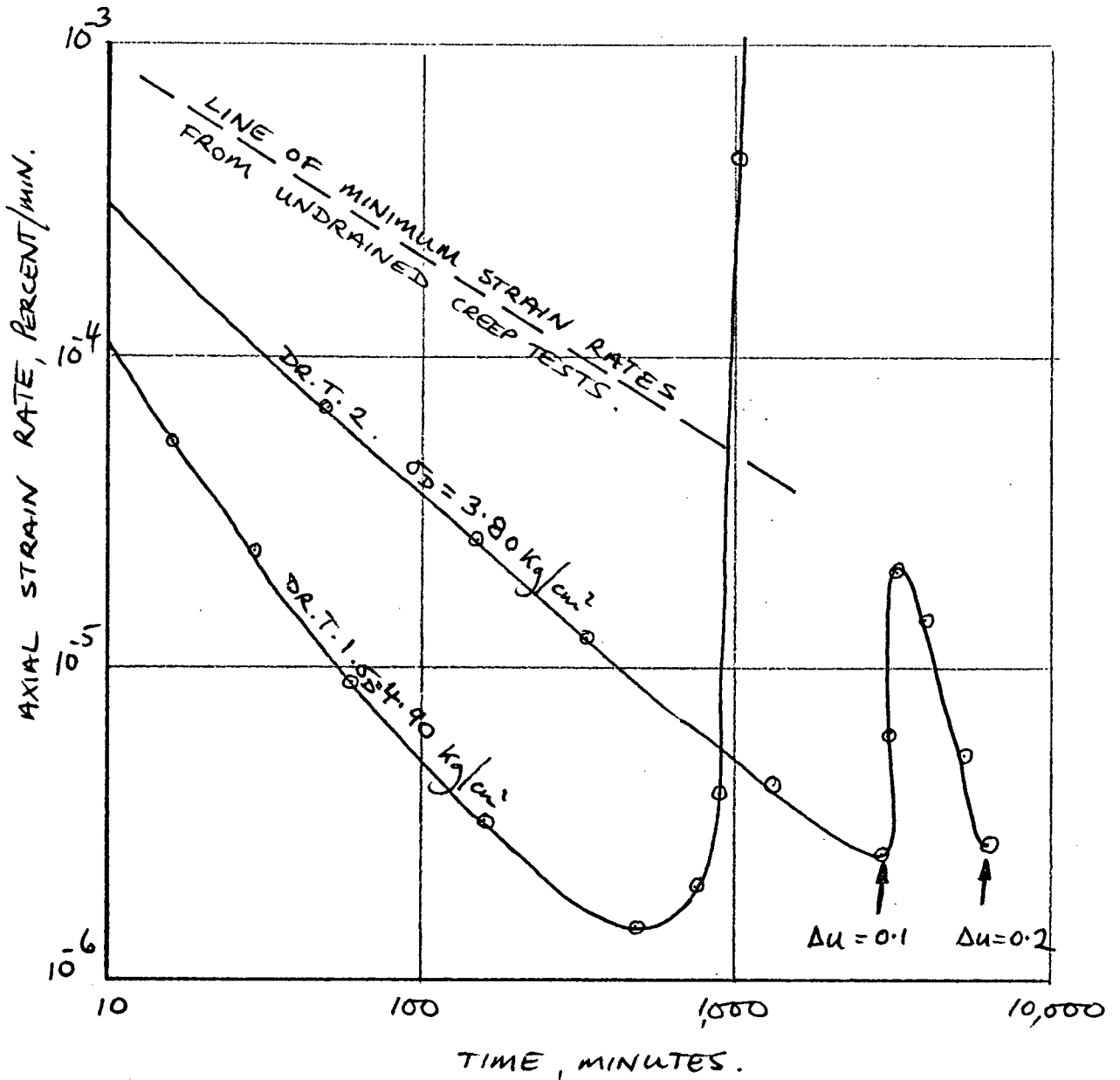


FIG. 31 CREEP RATE BEHAVIOUR FOR ISOTROPICALLY CONSOLIDATED DRAINED CREEP TESTS ON UNDISTURBED S.J.V. CLAY.

This indicates that the compression due to the stress level was being exactly compensated by the swelling due to the boost in pore pressure. After a total time of 9000 minutes the pore pressure was again boosted by 0.1 Kg/cm^2 , which put the sample under an effective stress of 0.1 Kg/cm^2 . The test was then continued for another 3000 minutes, after which time the sample had still not failed. This indicates how the strength of the sample is dependant almost completely on the bonding which appears to be independant of effective stress.

Table V shows a summary of the results of the creep tests. CR.T3 and CR.T8 have been omitted since they did not fail. Table V also shows that the strain reached at minimum strain rate ranged from 0.40 to 0.49 percent.

5.3 STRESS-STRAIN-STRAIN RATE RELATIONS.

Campanella and Vaid (1972) had found that for a given consolidation history there exists a unique stress-strain-strain rate law that could be used to correlate the results of creep and constant strain rate tests.

Figure 32 shows the constant stress creep rupture curves for some of the undrained tests on a log strain rate versus strain plot. A constant strain rate test is also shown on this plot by a horizontal line

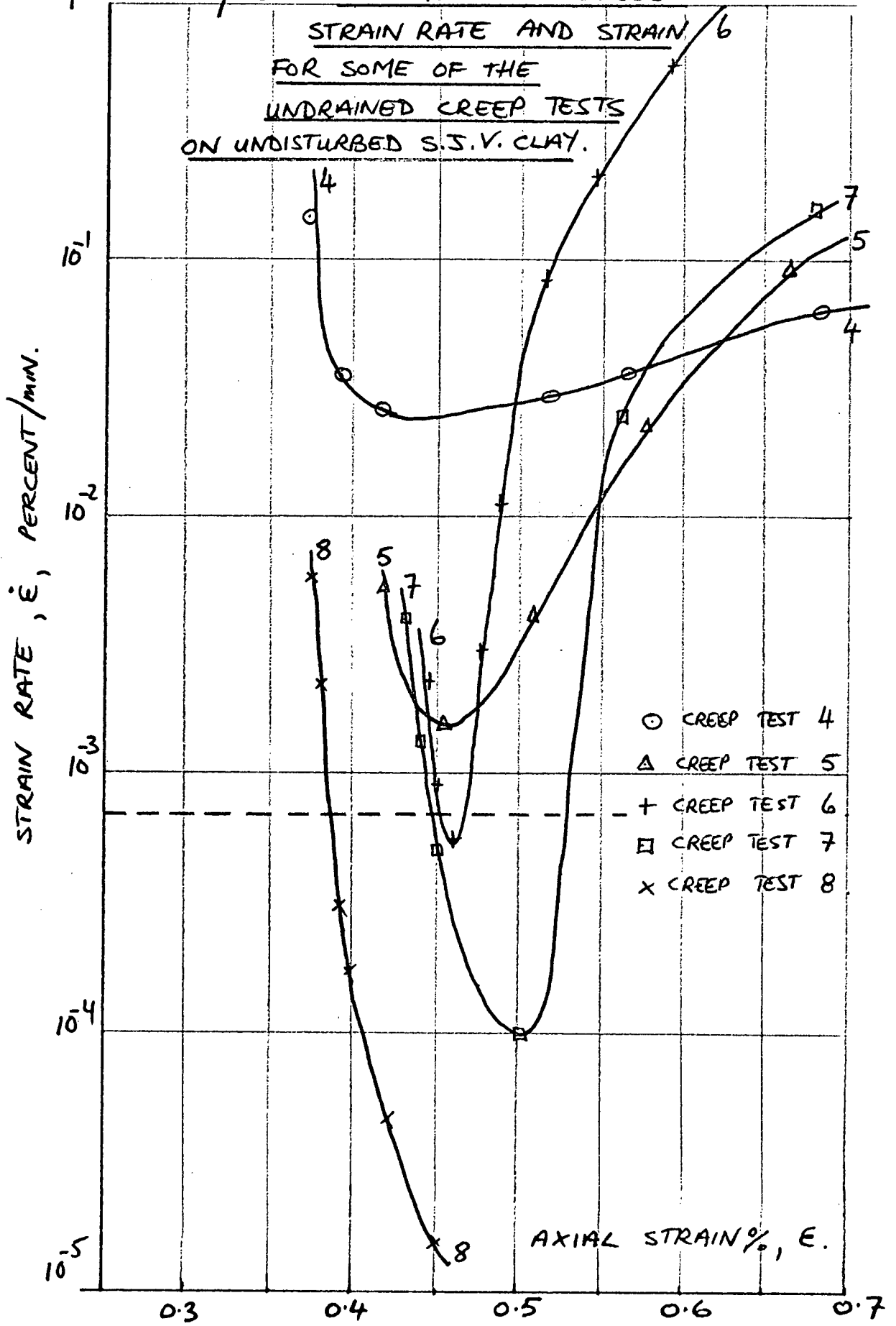
TABLE V

SUMMARY OF RESULTS OF
CREEP TESTS.

UNDRAINED

TEST No.	APPLIED STRESS $\bar{\sigma}_0$ (Kg/cm ²)	MEAN EFFECTIVE CONSOL. STRESS σ_m' Kg/cm ²	MINIMUM STRAIN RATE $\dot{\epsilon}_{min}$ %/min	STRAIN RATE AT, $\dot{\epsilon}_{min}$ %	RUPTURE LIFE, t_r mins
CR.T1	4.71	0.45	1.8×10^{-3}	0.40	40
CR.T2	4.32	0.42	1.2×10^{-4}	0.42	300
CR.T4	6.30	0.43	2.7×10^{-2}	0.42	10
CR.T5	5.97	0.47	1.5×10^{-3}	0.455	50
CR.T6	5.74	0.46	4.6×10^{-4}	0.46	135
CR.T6A	5.85	0.49	2.1×10^{-4}	0.47	120
CR.T7	5.50	0.43	8.9×10^{-5}	0.49	1050

FIG. 32 RELATIONSHIP BETWEEN STRAIN RATE AND STRAIN FOR SOME OF THE UNDRAINED CREEP TESTS ON UNDISTURBED S.S.V. CLAY.



corresponding to the value of the strain rate used. If the stress is assumed uniquely related to the current strain and strain rate, then the points of intersection of the constant strain rate test with the creep curves would give a set of values defining the stress - strain curve for that particular constant strain rate used.

The stress - strain curve determined from a constant strain rate test, having the same consolidation history as that used for the creep tests, is shown in Figure 33. The predicted stress-strain curve from the series of creep curves is also shown by the circles. It can be seen that reasonable agreement exists, except that the predicted points are shifted to one side by approximately 0.1%. Because of the very small range of strains encountered with this clay, this shift could well have been caused by a nonuniformity in the seating loads.

Snead (1970) and Campanella and Vaid (1972) both restricted the use of a unique stress strain-strain rate relationship to soils tested undrained at constant temperature and not heavily overconsolidated, where as these results would indicate that this relationship could still be applied to a heavily overconsolidated and bonded clay.

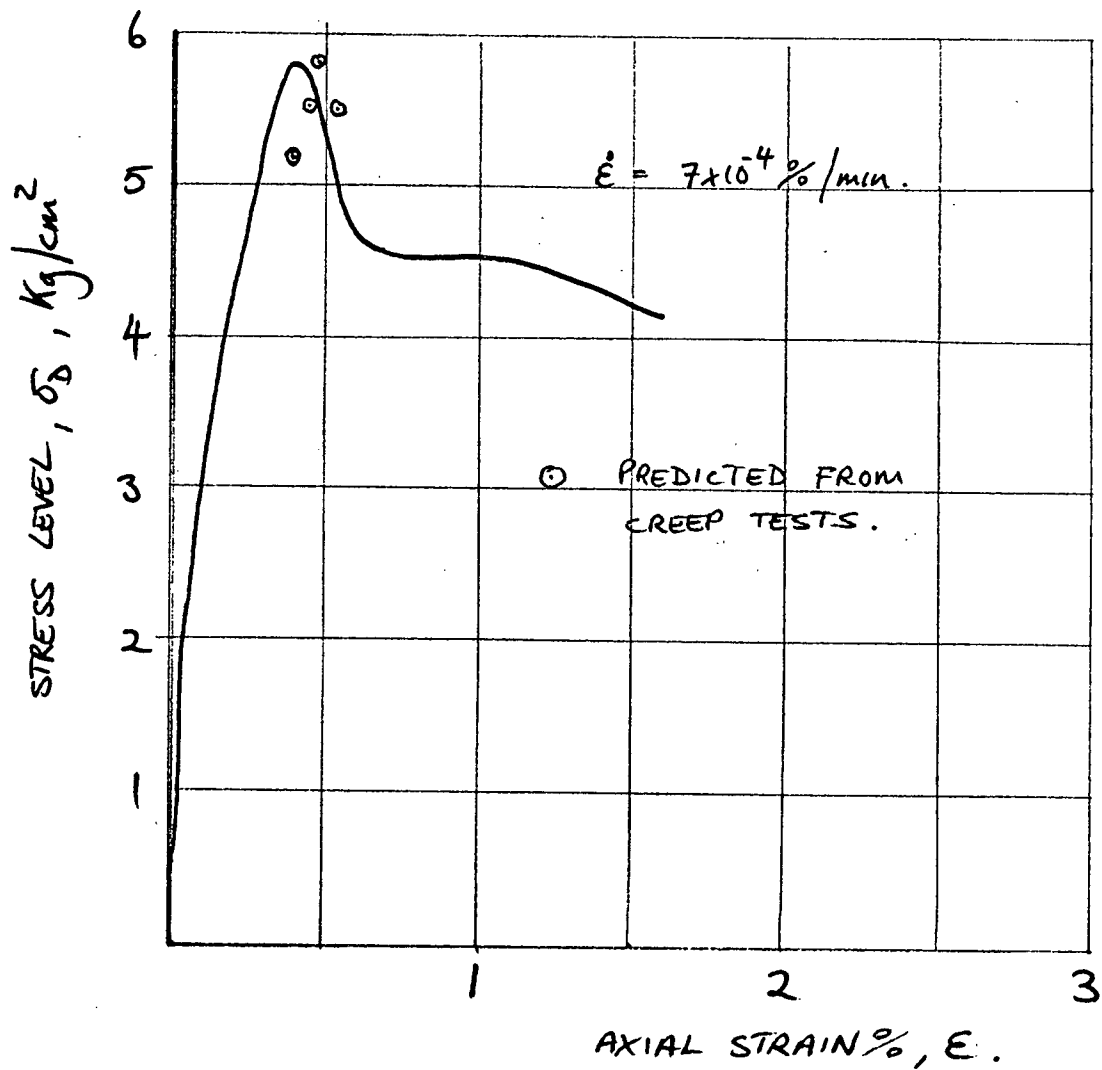


FIG. 33. COMPARISON OF OBSERVED STRESS - STRAIN BEHAVIOUR IN UNDRAINED CONSTANT STRAIN RATE COMPRESSION TESTS WITH THAT PREDICTED FROM UNDRAINED CREEP TESTS.

5.4 EFFECTIVE STRESS CONDITIONS.

Figure 34 shows the effective stress conditions of the undrained creep tests at the instant of minimum creep rate on a modified Mohr plot. All the points lie very close to the line of limit for triaxial testing, where the effective confining stress, σ'_3 , equals zero. Comparison of this plot with the equivalent plot for the undrained strain controlled compression tests, Figure 23, shows that the instant of peak deviator stress is also defined by the same envelope. These points could have fallen onto this same line simply because the tests had all reached their limit for triaxial testing, that is, the pore pressure equalled the cell pressure. But in the undrained/drained strain controlled compression test, where the drainage valve was opened just after peak deviator stress, the effective stress within the sample was not zero at peak, but this point still plots very close to the envelope. This indicates that there could be a single envelope for peak deviator stress in the strain controlled compression tests and minimum creep rate in the creep tests.

Campanella and Vaid (1972) found that the linear envelope defined by the instant of minimum creep rate occurred at a lower shearing resistance than that defined by the strain controlled compression tests.

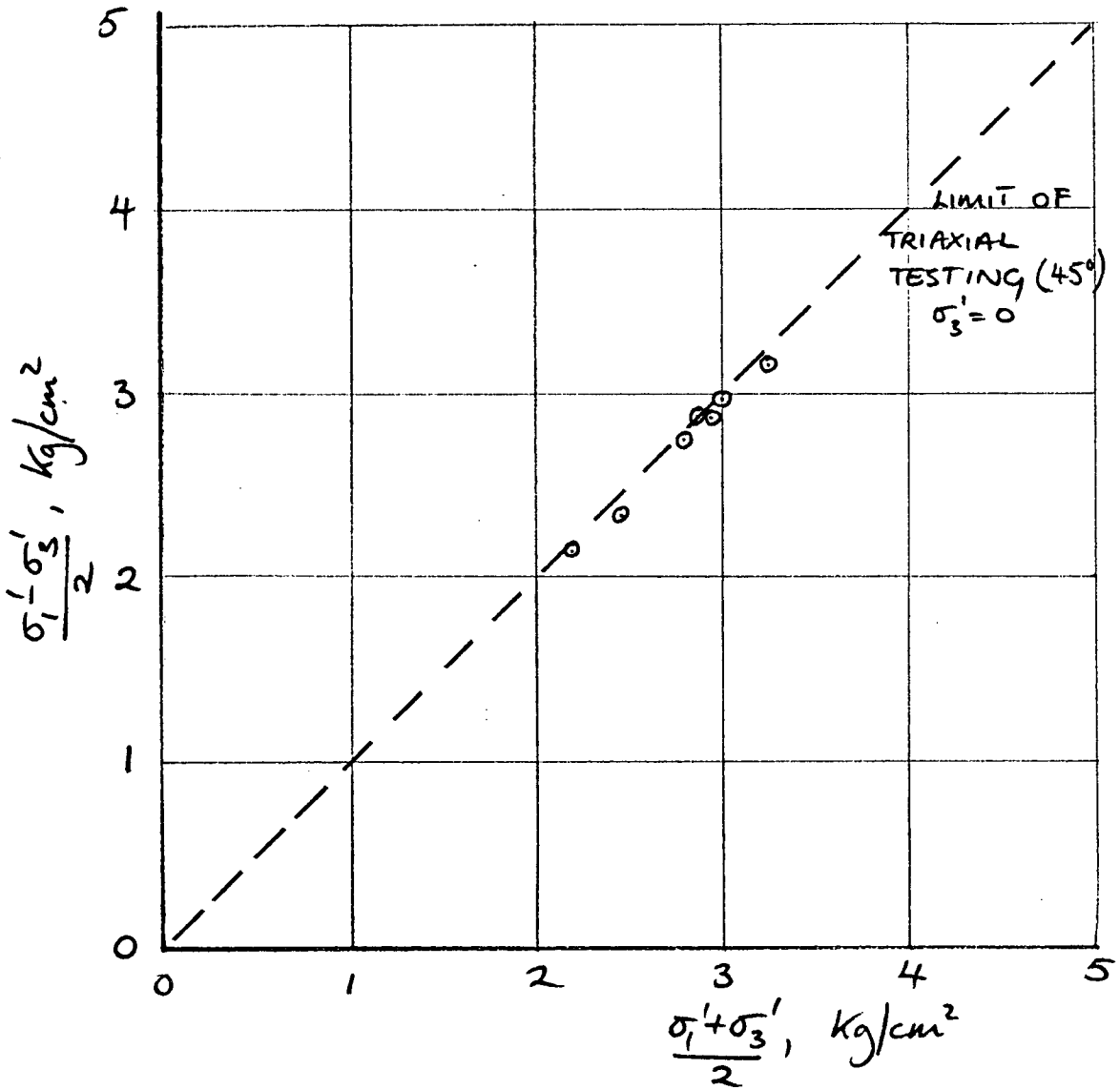


FIG. 34. EFFECTIVE STRESS CONDITIONS
AT MINIMUM CREEP RATE FOR
THE UNDRAINED CREEP TESTS
ON UNDISTURBED S.S.V. CLAY.

This difference in results is chiefly due to the fact that the results herein are for a heavily overconsolidated, cemented clay, whereas those obtained by Campanella and Vaid were for a normally consolidated clay.

CHAPTER 6

SUMMARY AND CONCLUSIONS

The testing of this very stiff, sensitive clay was very difficult since the axial strains to failure were very small, all less than 1 percent.

Based on the uniaxial constant stress creep rupture tests and the strain controlled compression tests certain conclusions can be drawn. There appears to exist a linear relationship between log minimum creep rate and log rupture life and also log minimum creep rate and log remaining time to rupture. A linear relationship was also noted between log current creep rate during tertiary creep and the remaining time to rupture, although very little reliance can be placed on strains measured near to creep rupture. A linear relationship between log minimum creep rate and stress level and a possible link between stress and strain rate for both strain controlled compression tests and creep tests appears to exist. There is some indication that a stress-strain-strain rate relationship may exist for this over-consolidated, cemented clay.

Results from the Ko consolidation tests, performed by Dr. Y.P.Vaid, show that the apparent pre-consolidation pressure varies over a very large range, if

tested at different strain rates.

In conclusion, the results obtained in this research were very dependant on the bonding that existed in this clay, and that the bond strength appeared to be a function of the strain rate.

BIBLIOGRAPHY

1. Bishop, A.W., Henkel, D.J., (1962), "The measurement of soil properties in the triaxial test." Edward Arnold, Second Edition.
2. Campanella, R.G., and R.C. Gupta, (1966), "Effect of Structure on Shearing resistance of a sensitive Clay." Soil Mechanics Series No. 6 U.B.C.
3. Campanella, R.G., and Y. Vaid, (1972), "Creep rupture of a saturated Natural Clay." Soil Mechanics Series No. 16 U.B.C.
4. Campanella, R.G., and Y. Vaid, (1973), "Triaxial and Plane Strain Creep Rupture of an undisturbed Clay," Soil Mechanics Series No. 21, U.B.C.
5. Casagrande, A., and S. Wilson, (1951), "Effect of rate of loading on strength of clays and shales at constant water content." Geotechnique, Vol. II, No. 3, June 1951.
6. Conlon, R.J., (1966), "Landslide on the Toulmoustouc River, Quebec." Canadian Geotechnical Journal, Vol.
7. Crawford, C.B., (1959). "The influence of rate of strain on effective stresses in sensitive clay." ASTM, STP. No. 254.
8. Crawford, C.B., (1968), "Quick Clays of Eastern Canada." Engineering Geology, Amsterdam, pp. 239-265.
9. Gadd, N.R., (1962), "Surficial geology of Ottawa map-area Ontario and Quebec." Geol. Surv. Can., Paper, 62(16): 4 pp.
10. Haefeli, R., (1953), "Creep problems in Soils, Snow and Ice." Proceedings, 3rd. Int. Conf. on soil Mech. and Found. Eng., Vol. III, pp. 238-251, 1953.

11. Henkel, D.J., (1957), "Investigation of two long term failures in London clay slopes at Wood and Northolt." Proceedings 4th Int. Conf. on S.M. and Found. Eng., Vol. II, p. 315, 1957.
12. Kenney, T.C., and L. Bjerrum, (1972), "Effect of structure on the shear behaviour of Normally consolidated Quick Clays." Canadian Geotechnical Vol. 9. No. 3 1972.
13. Loiselle, A., M. Massiera, and U.R. Sainani, (1970) "A Study of the Cementation Bonds of the Sensitive clays of the Ontario River Region." Can. Geotechnical Journal, Vol. 8.
14. Lubahn, J.D. and R.P. Felgar, (1961), "Plasticity and creep of metals." J. Wiley and Sons Inc., New York, p. 600.
15. Mallawaratchie, D.P., (1970), "Plane strain creep rupture of a saturated undisturbed clay." M.A.Sc. Thesis U.B.C.
16. Mitchell, J.K., A. Singh, and R.G. Campanella, (1969) "Bonding, Effective stresses, and strength of soils." Jour. of S.M. and Found. Div. ASCE, Vol. 95, S.M. 5, pp. 1219-1246.
17. Saito, M., and H. Uezawa, (1961), "Failure of soil due to creep." Proceeding of the 5th Int. Conf. on S.M. and F.E., Paris, Vol. I pp. 315-318.
18. Saito, M., (1969), "Forecasting time of slope failure by tertiary creep." Proc. 7th Int. Conf. on S.M. and F.E., Mexico, Vol. II, pp. 677-683.
19. Sead, D. (1970), "Creep studies on an undisturbed sensitive clay." Ph.D. Thesis, U.B.C.
20. Suklje, (1961), "A landslide due to long term creep." Proceedings 5th Int. Conf. on S.M. and F.E. VOL II, p. 727, 1961.

21. Tavenas, F., J.Y. Changnon, and P. LaRochelle, (1971), "The Saint-Jean-Vianney Landslide: Observations and eyewitnesses Accounts." Can. Geotechnical Journal, Vol. 8 pp. 463-478.
22. Townsend, D.L., D.L. Sangrey, and I.K. Walker, (1969) "The Brittle Behaviour of naturally cemented soils." Proc. 7th Int. Conf. S.M. and F.E. Mexico pp. 411-417.
23. Vialor, S., and A. Skibitsky, (1957), "Rheological processes in frozen soils and dense clay." Proc. 4th Int. Conf. on S.M. and F.E., Vol. I, p 121. 1957.

APPENDIX I

CALCULATION OF STRAIN RATES

The strain rates were computed by using the strain-log time plot as shown in Figure A1. A smooth curve was drawn through the strain-log time points plotted from the "raw" data. The technique to calculate strain rates assumes a linear change in strain for finite time intervals. The strain rate at a given time "t" was determined by subtracting the value of the strain at (t- Δt) from the value at t+ Δt and divided by time interval Δt (Figure A1). That is the strain at B (Figure A1) was taken to be:

$$= \frac{\text{Strain ordinate at C} - \text{strain ordinate at A}}{\text{time AC (natural scale)}}$$

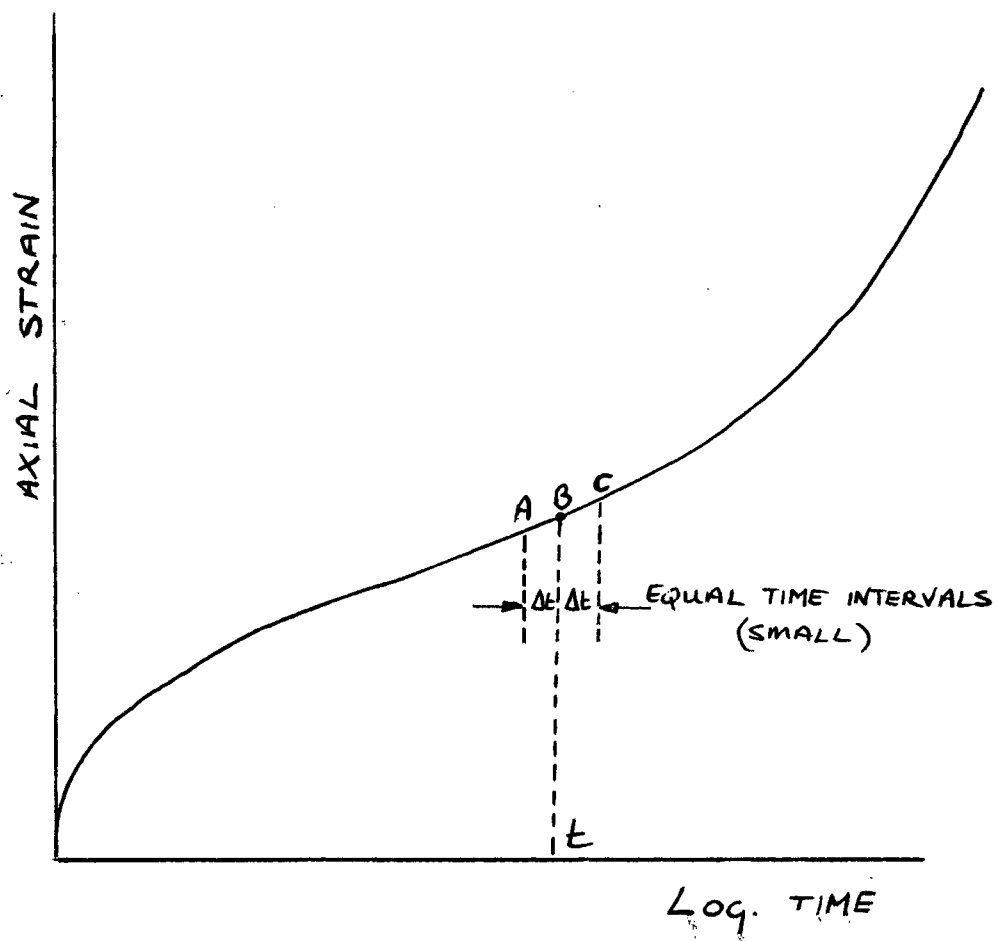


FIGURE. A1. CALCULATION OF STRAIN RATES.

APPENDIX II

SKETCHES OF FAILED SAMPLES

UD1



UD2



UD3



UD4



UD5



UD6



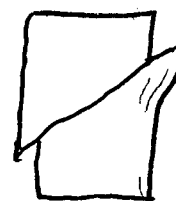
CR.T1



CR.T2



CR.T4



CR.T5



CR.T6



CR.T7

